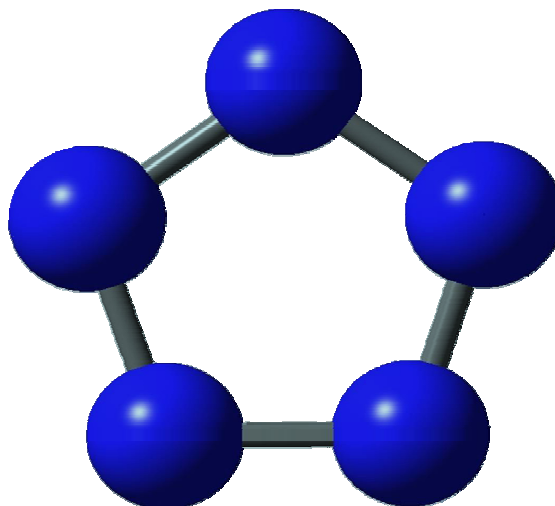


Sara Wallin, Henric Östmark, Tore Brinck, Peter Carlqvist, Rob Claridge, Lars Eriksson, Arno Hahma, Emma Hedlund, Erik Holmgren, Martin Norrefeldt, Larisa Yudina

High Energy Density Materials Efforts to synthesize the pentazolate anion: Part 1



SWEDISH DEFENCE RESEARCH AGENCY

Weapons and Protection

SE-147 25 Tumba

FOI-R--1602--SE

March 2005

ISSN 1650-1942

Technical report

Sara Wallin, Henric Östmark, Tore Brinck, Peter Carlqvist, Rob Claridge, Lars Eriksson, Arno Hahma, Emma Hedlund, Erik Holmgren, Martin Norrefeldt, Larisa Yudina

High Energy Density Materials Efforts to synthesize the pentazolate anion: Part 1

Contents

1	Executive abstract in Swedish / Sammanfattning	4
1.1	Inledning.....	4
1.2	Syntes av N_5^-	4
1.2.1	Varför N_5^- ?	5
1.2.2	Metallkomplex	5
1.2.3	Grundläggande studier av arylpentazoler.....	6
1.2.4	Detektion av N_5^- i masspektrometer.....	7
1.2.5	En våtkemisk väg till N_5^- ?.....	7
1.2.6	Slutsats	8
2	Introduction	9
3	Roadmap to pentaaza HEDM:s	12
3.1	First step: Detection of the pentazolate anion	12
3.2	Second step: Stable pentazolate salts or metal complexes.....	13
3.3	Third step: Ion exchange	14
4	Starting materials.....	17
4.1	Synthesis of various starting materials.....	17
4.1.1	Synthesis of <i>p</i> -dimethylaminophenylpentazole	19
4.1.2	Synthesis of <i>p</i> -methoxyphenylpentazole.....	21
4.1.3	Synthesis of <i>p</i> -tertbutylphenylpentazole	22
4.1.4	Synthesis of <i>p</i> -nitrophenylpentazole	22
4.1.5	Salts of <i>p</i> -pentazolephenylsulfonic acid.....	23
4.1.5.1	A stable diazonium salt of <i>p</i> -pentazolephenylsulphonic acid	24
4.1.5.2	Sodium, potassium and barium salts of <i>p</i> -pentazolephenylsulphonic acid..	27
4.2	The stability of arylpentazoles, QM calculations.....	29
4.2.1	Calculated activation energies.....	29
4.2.2	Effect of the TS structure on stability	30
4.2.3	Ortho substituted <i>p</i> -aminophenylpentazole.....	31
4.2.4	Implications for the benzyne mechanism.....	32
4.2.5	The stability of tetrazolpentazoles.....	33
5	Detection	35
5.1	Raman and IR absorption spectroscopy	35
5.2	CARS – Coherent Anti-Stokes Raman Scattering.....	36

5.3	NMR spectroscopy	37
5.3.1	Reaction kinetics measurements with ^1H -NMR.....	37
5.3.2	^{15}N - and ^{14}N -NMR, theoretical calculations	40
5.4	UV spectroscopy	42
5.5	Mass spectrometry.....	43
5.5.1	Electrospray ionization.....	43
5.5.2	Laser Desorption, Electron Impact Ionization with a CO_2 laser	44
5.5.3	Laser Ionization.....	47
5.5.3.1	Experimental setup.....	47
5.5.3.2	Calibration.....	49
5.5.3.3	Results	50
5.5.3.4	QM calculations	53
5.5.3.5	Discussion and conclusions.....	54
5.5.3.6	Future experiments.....	55
6	Benzyne reaction or amination of arylpentazoles	56
6.1	The proton transfer step.....	56
6.2	Benzyne formation	58
6.3	Lowering the activation energy with metal complex	60
7	Conclusions	61
8	References	62

1 Executive abstract in Swedish / Sammanfattning

1.1 Inledning

Det forskningsområde inom energetiska material som kallas High Energy Density Materials, HEDM, d.v.s energetiska material med väsentligt högre prestanda (för explosivämnestillämpningar bättre än eller likvärdig med CL-20), beskrevs nyligen ingående i rapporten ”*High Energy Density Materials (HEDM) - A literature survey*” [1]. Detta var en litteraturstudie vilken beskrev läget i världen inom HEDM-området och avhandlade möjligheterna att utveckla HEDM, samt visade på möjlig potential och tidsperspektiv. I rapporten gavs även en utförlig översikt över det internationella läget och en kort genomgång av vad som görs på FOI inom detta område.

FOI är en av världens ledande forskningsgrupper inom HEDM-området och ledande i Europa vilket visar sig bl. a. genom att FOI har blivit ombett att för CEPA-14 hålla i en konferens om HEDM. Den nyss nämnda rapporten kommer att ligga till grund för arbetet på HEDM inom CEPA-14. Dessutom har FOI under flera år haft samarbete med Storbritannien där de skickar sina forskare till Institutionen för Energetiska Material under några månader för att bedriva forskning inom HEDM.

Föreliggande rapport redovisar och dokumenterar en del av det praktiska arbetet med att framställa HEDM som görs på FOI. Den tekniska delen av rapporten är skriven på engelska för att kunna användas som diskussionsunderlag i kontakter med andra som arbetar inom samma område då dessa uteslutande finns utomlands.

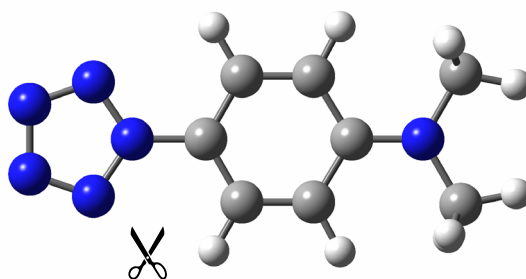
1.2 Syntes av N_5^-

Föreliggande rapport redovisar resultat från forskningen på FOI om helkväveföreningar vilka har stort intresse som HEDM. Närmare bestämt handlar rapporten om försök att göra *cyclo-N₅⁻*. Försök att syntetisera denna jon gjordes redan för femtio år sedan då tyska forskare, Ugi och Huisgen, studerade s.k. arylpentazoler, föreningar med en femring av kväven som sitter på en bensenring tillsammans med eventuella andra substituenten (Figur 1), och

möjligheten att bryta loss kväveringen från molekyl. Under senare år har denna idé rönt förnyat intresse då nya och/eller bättre analysmetoder och inte minst beräkningsmetoder finns tillgängliga idag.

1.2.1 Varför N_5^- ?

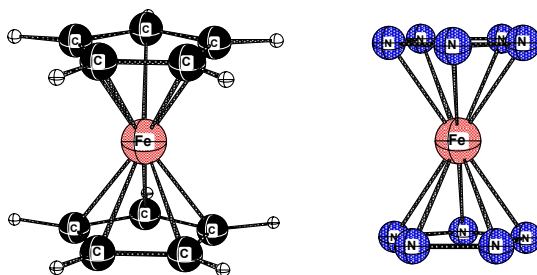
Intresset för att göra N_5^- grundar sig på beräkningar av jonens egenskaper såsom stabilitet och möjlig prestanda tillsammans med en positiv jon såsom t.ex. N_5^+ . Som framgår av Table 1 i kapitel 2 "Introduction" på sidan 11 skulle $N_5^+N_5^-$ som sprängämne vara 1.6 gånger så bra som HMX och som drivämne ha mycket hög specifik impuls (räknat som rent ämne). Det är svårt att avgöra huruvida $N_5^+N_5^-$ som förening skulle vara stabil eller inte. Olika grupper har kommit fram till olika resultat i frågan. Enigheten är dock total om att det skulle vara ett fantastiskt sprängämne eller drivämne om det kan göras i stabil form.



Figur 1 Den mest stabila och lätthanterliga arylpentazolen, *p*-dimethylaminophenylpentazol.

1.2.2 Metallkomplex

För att åstadkomma ett stabilt salt av N_5^- är tanken att fånga jonen i ett metallkomplex. Liknande komplex med cyclopentadienjoner (C_5H_5), dvs. motsvarande kolring (med ett väte på varje kol) vilken har stora kemiska likheter med *cyclo*- N_5^- , är mycket stabila föreningar. Ett exempel är ferrocene (Figur 2). Beräkningar visar att motsvarande kväveförening är nästan lika stabil.

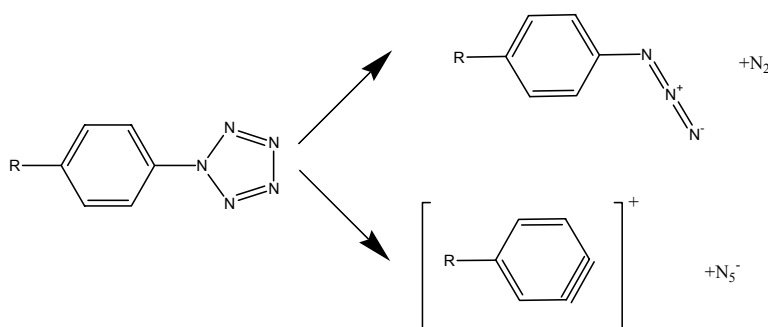


Figur 2 Ferrocene och dess motsvarande kväveförening

Metallsaltet förväntas i sig inte vara särskilt energetiskt. Däremot är det ett utmärkt steg på vägen mot t.ex. $N_5^+N_5^-$ eller ett salt med någon annan positiv jon vilket kan åstadkommas genom ett jonbyte. Mycket forskningsarbete om metallkomplex med N_5^- finns redovisat i litteraturen och arbete pågår på FOI, både teoretiskt och experimentellt, på metallkomplex med arylpentazoler och N_5^- . Detta arbete kommer att redovisas i framtida rapporter.

1.2.3 Grundläggande studier av arylpentazoler

För att lägga en bra grund för att bryta av N_5 -ringen från arylpentazoler behövs ingående kunskaper om arylpentazolers egenskaper. Därför har vi studerat arylpentazoler både teoretiskt och experimentellt. Den i huvudsak konkurrerande sönderfallsvägen för arylpentazoler är att släppa N_2 från kväveringen så att det bara blir tre kväven kvar – alltså motsvarande arylazid. Detta sönderfall sker alltid hos arylpentazoler och i högre grad vid högre temperaturer. Olika arylpentazoler är olika känsliga för värme. De mest instabila sönderfaller snabbt redan vid temperaturer långt under 0°C . En av de mest stabila, *p*-dimethylaminophenylpentazole är stabil nog att hanteras om den förvaras kallt (i flytande kväve) och överförs med kalla spatlar och till kylda kärl. Detta är därför den arylpentazol vi oftast använder vid försök att göra N_5^- .



Figur 3 Konkurrerande sönderfall av arylpentazoler.

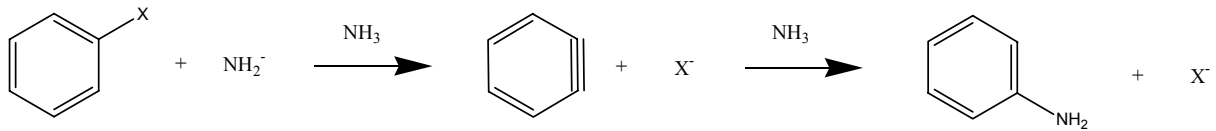
Flera arylpentazoler har studerats experimentellt och med kvantmekaniska beräkningar. Det är önskvärt att hitta en arylpentazol som är så stabil som möjligt mot att släppa N_2 , men som har en försvagad bindning mellan de två ringarna och alltså har lättare att släppa N_5^- .

1.2.4 Detektion av N_5^- i masspektrometer

Under 2003 lyckades vi på FOI med uppgiften att påvisa att det är möjligt att bryta loss kväveringen från arylpentazoler och att N_5^- dessutom är stabil, åtminstone under vissa speciella förutsättningar (kort tid och i gasfas i vakuum). Detta gjordes genom att med laserljus slå sönder molekylerna och jonisera fragmenten och sedan detektera dessa med en Time-of-Flight masspektrometer. Beräkningar visar att jonen ska vara relativt stabil och det långsiktiga målet är att isolera den tillsammans med en lämplig positiv jon, i lösning eller fast form. Att påvisa jonens existens i masspektrometerexperiment måste betraktas som ett av de två stora genombrott som skett inom helkvävekemin de senaste hundra åren. Det andra är syntesen av N_5^+ som gjordes av Karl Christe vid Edwards Air Force Base i USA 1998. Att syntetisera jonen i lösning eller i fast form skulle givetvis vara ett ännu större genombrott.

1.2.5 En våtkemisk väg till N_5^- ?

För att syntetisera N_5^- i lösning eller i fast form behövs ett annat sätt än laserljus för att bryta bindningen. En sådan väg är nukleofil aromatisk substitution med natriumamid. Reaktionen (Figur 4) går ut på att NH_2^- används för att "byta ut" en substituent (molekyldel) på en bensenring till NH_2 genom att släppa iväg den ursprungliga substituenten (negativt laddad). Detta är en välkänd reaktion då halogenerna brom och klor byts ut medan reaktionen inte fungerar för fluor. Kvantmekaniska beräkningar har nu gjorts för att se om reaktionen kan fungera för att byta ut N_5 . Dessa visar att det är lite lättare att byta ut N_5 än fluor, men att det troligen krävs för mycket energi under normala förhållanden. De visar dock också på ett knep som skulle kunna få reaktionen att fungera, nämligen att använda zinkjoner för att bilda ett komplex med N_5 så att det är *cyclo*- $N_5 \cdots Zn^{2+}$ som ska bytas ut istället. Detta minskar energin som krävs så att reaktionen sannolikt är möjlig.



Figur 4 Nukleofil aromatisk substitution med natriumamid. $X = \text{Br}, \text{Cl}$ eller $\text{cyclo-N}_5 \cdots \text{Zn}^{2+}$.

1.2.6 Slutsats

Prestandan hos N_5^- måste bedömas för ett salt med en specifik motjon såsom N_5^+ . N_5^+N_5^- som sprängämne skulle vara 1.6 gånger så bra som HMX och som drivämne ha mycket hög specifik impuls (räknat som rent ämne)

Arbetet med att göra N_5^- går mycket bra. Ett genombrott har åstadkommit genom dess detektion i en masspektrometer och arbetet fortsätter mot att framställa den i form av ett metallsalt i lösning eller fast form.

Arbetet med att göra metallsalt med N_5^- pågår och mer om denna forskning kommer att redovisas i framtida rapporter.

2 Introduction

Polynitrogen compounds have received considerable attention in recent years as potential candidates for high energy density materials (HEDMs). The fact that most of these have a very high calculated energy content is a consequence of the large bond energy of 228 kcal/mol of the triple bond in molecular nitrogen (N_2) compared to the bond energies of nitrogen-nitrogen single and double bonds, which typically amounts to 39 and 100 kcal/mol, respectively. In addition to the favorable energetics of the polynitrogen compounds, they also have the advantage that the energy releasing decomposition into N_2 leads to no deposition of harmful substances. This makes them particularly suitable for propulsion of spacecrafts, since the commonly used propellants of today results in large depositions of harmful substances in the atmosphere. The special properties of polynitrogen compounds also make them of great interest for energy storage. The high heat of formation and large density makes polynitrogens nearly ideal for use as high explosives.

Theoretical calculations lay the foundation for ongoing attempts to synthesise all-nitrogen compounds and increases the possibility of successfully producing one or a few useful substances and formulations. A possible development in this field is substances allowing an increase in performance as high explosives of 2–5 times the values of today (Table 1). The impulse of for example N_4 is comparable to H_2/O_2 but has the enormous advantage of a much higher density which would allow for smaller and thereby lighter rockets.

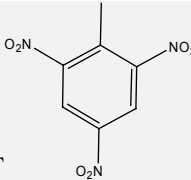
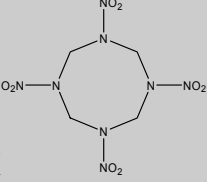
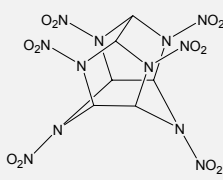
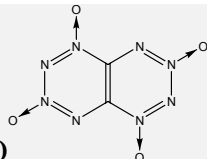
Even though theoretical studies have identified a number of potentially stable structures, the experimentally observed nitrogen compounds are still few. The azide anion, N_3^- , was first synthesized in 1890 by Curtius. Christe and coworkers have since 1999 reported the preparation and isolation of N_5^+ together with several different counter ions [2]. A few other species, such as N_3 , N_3^+ and N_4^+ , have been observed only as gaseous or matrix-isolated ions or radicals. The formation of N_5^- from arylpentazoles in mass spectrometry experiments has recently been reported from our lab [3, 4] and from Air Force Research Laboratory (Edwards Air Force Bas) in the US [5]. The detection of HN_5 and a zinc pentazolate salt in solution has also been reported [6].

The nitrogen pentazole ring system has been studied since 1903, when Hantzsch made the first attempts to prepare phenylpentazole [7]. The first preparation of substituted pentazoles was however achieved by Huisgen and Ugi [8] in 1956. Calculations have shown that the

aromatic pentazole anion (N_5^-) should be stable enough to isolate, especially if trapped as a metal complex [9-14]. This complex could, if a suitable metal were used as the complexing agent, be highly energetic. More important, it could serve as a N_5^- -containing compound, stable enough for an ion exchange to be performed.

The area of High Energy Density Materials was recently reviewed in a report, "*High Energy Density Materials (HEDM) - A literature survey*" [1]. This was a literature study which described the current status worldwide and treated the possibilities to develop HEDM as well as the possible potential and time perspectives.

Table 1 Comparison of performance for common high explosives, high nitrogen compounds and some theoretical HEDMs, calculations using Cheetah 2.0 with BKWC EOS.

Energetic material	Density (g/cc)	Heat of formation (kJ/mol)	Detonation velocity (mm/ μ s)	Detonation pressure (GPa)	Energy (HMX=100, V=2.2 V ₀)	Energy (HMX=100, V=40 V ₀)	Impulse (s)	Force (J/g)
<i>Reference compounds:</i>								
NC, Nitrocellulose	1.65	-708	7.3	21.2	60	65	226	992
 TNT	1.65	-63	6.9	19.6	55	63	210	897
 HMX	1.905	74.75	9.1	38.5	105	103	266	1397
 CL-20	2.04	393	10	47.8	121	116	273	1380
<i>HEDM:</i>								
N ₅ ⁺ N ₅ ⁻	1.9	1239	12.1	62	162	156	347	~2000 ^b
 N ₄ (T _d)	2.3	761	15.5	121	308	288	422	3700
N ₆₀	1.97	6780	12.3	65	161	150	331	2296
Poly-N	3.9	290	30	660	1060	- ^a	513	- ^a
 TTTO	2.38	795	10.9	131	220	- ^a	288	- ^a

^a Calculations do not converge.

^b Old calculations with slightly different conditions. The new calculations do not converge.

3 Roadmap to pentaaza HEDM:s

The making of High Energy Density Materials with five-membered nitrogen rings starts with decomposition of arylpentazoles (Figure 1). This is not a new idea. As early as in the late 1950s, Ugi and Huisgen synthesized and studied the stability of arylpentazoles and tried to isolate the pentazolate anion from them. Recently a renewed interest in this ion has prompted new studies of these molecules using advanced quantum chemical calculations and new analysis methods that were not available fifty years ago as help. A breakthrough was achieved when the feasibility of this process was confirmed in a laser induced mass spectrometry experiment[3].

3.1 First step: Detection of the pentazolate anion

The making and detection of the pentazolate anion in any form is the first step on the road to pentaaza HEDM:s. This first step was taken in the spring of 2003 by the detection of *cyclo-N₅⁻* in a Laser Ionization Mass Spectrometry (LI-MS) experiment[3] which has been thoroughly described in previous reports[15]. This is an important result since it shows that the ion is stable, at least in vacuum and on the relatively short timescale of a few microseconds.

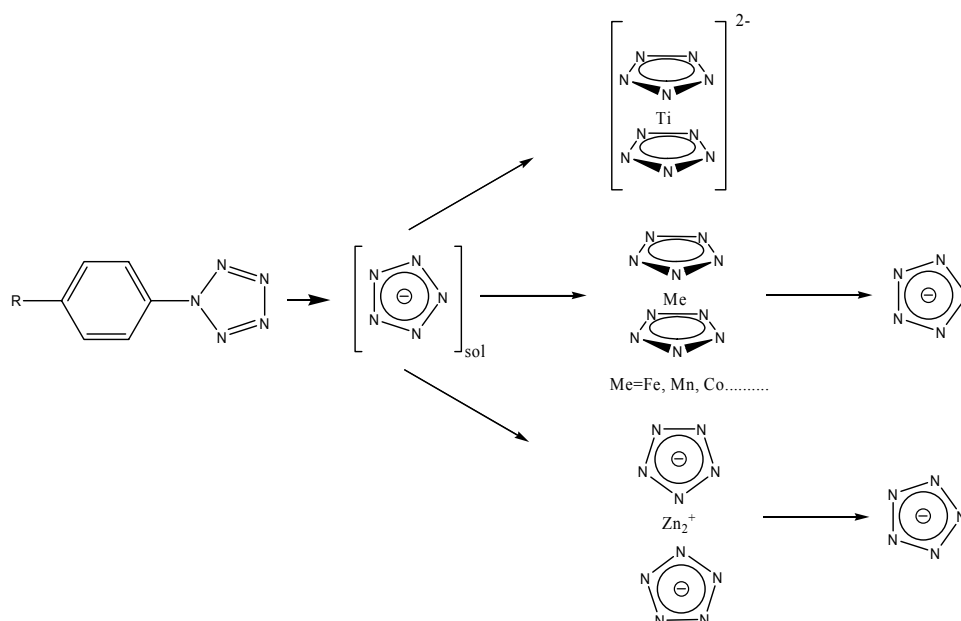


Figure 1 *How to make pentaaza HEDM's.*

3.2 Second step: Stable pentazolate salts or metal complexes

In order to make a stable compound, the primary goal is to make a neutral metal complex. QM calculations show that using for example Fe^{2+} , Mn^{2+} , and Cr^{2+} lead to ferrocene type complexes whereas for example Mg^{2+} , Ca^{2+} , Zn^{2+} forms an end-on type complex (Table 2, Figure 2). In a recently published article[16] proof of the existence of the $\text{Ti}(\eta^5\text{-P}_5)_2^{2-}$ complex was presented. The possibility of such a complex with the pentazolate anion has also been investigated[17] and found to be a reasonable assumption.

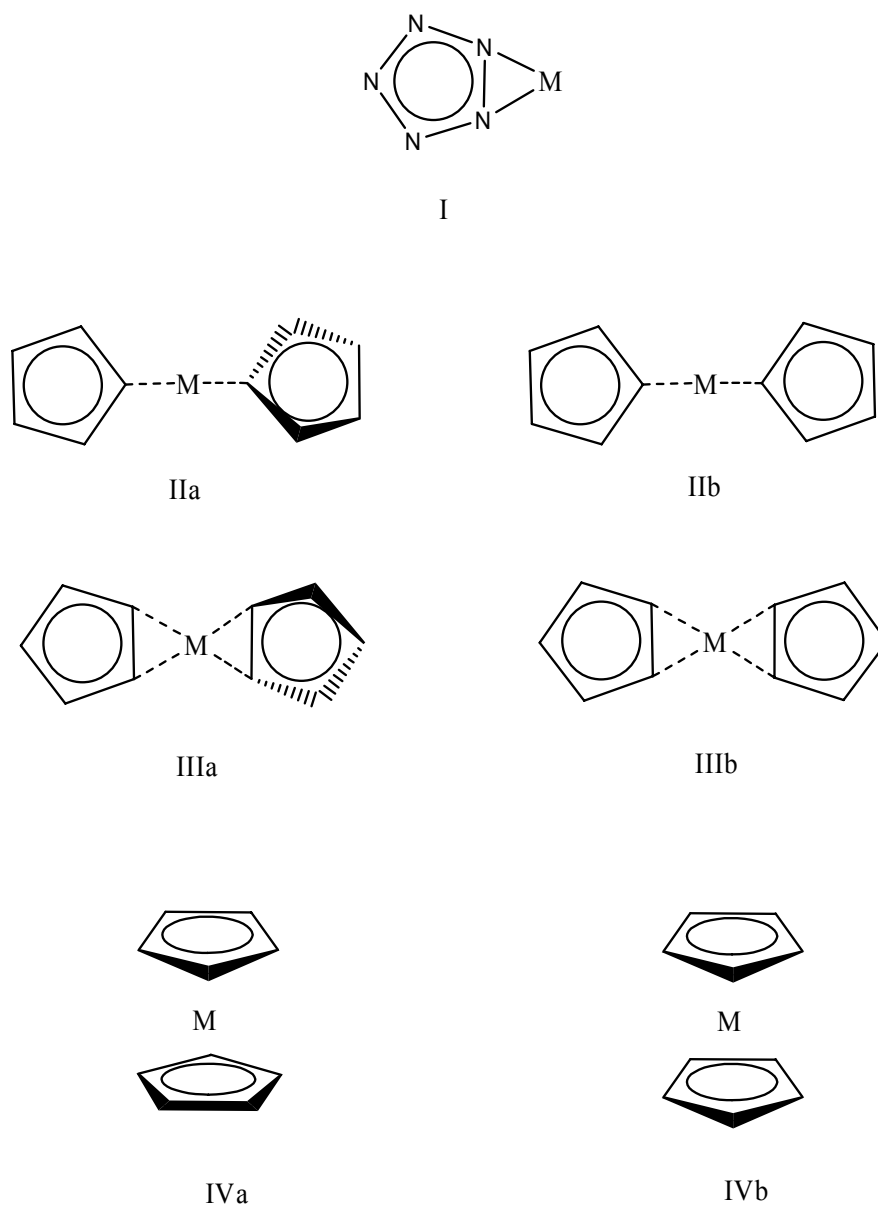


Figure 2 *Various structures of metal-pentazolate complexes from the literature. M=Metal*

Table 2 *Calculated structures of the metal complexes formed with pentazolate anions. Structure type refers to Figure 2.*

Metal	Structure	Reference
Li	I	Glukhovtsev [18]
Fe	IVa	Lein [12], Tsipis [14]
Mg	IIIa (IIIb)	Burke [11]
Na	IIIa	Burke [11]
K	IIIa (IVa)	Burke [11]
Ca	IIIa (IIIb)	Burke [11]
Zn	IIa (IIb)	Burke [11]
V	IVb	Tsipis [14]
Cr	IVa	Tsipis [14]
Mn	IIIa	Tsipis [14]
Co	IVa	Tsipis [14]
Ni	IVa	Tsipis [14]

Structures in paranthesis are not lowest in energy but too close in energy to be excluded as possible structures.

3.3 Third step: Ion exchange

Once a stable complex with N_5^- has been made, an ion exchange can be attempted in order to find a suitable counter ion that makes a good HEDM. Calculations show that a salt with the recently discovered[2] N_5^+ ion would be highly energetic, with a performance as an explosive about 1.6 times that of HMX[15], provided of course that it is stable. QM calculations on the stability of $N_5^+N_5^-$ are not conclusive. There are three studies of its stability, two of which predict that $N_5^+N_5^-$ is stable and one that predicts its instability.

The first publication, by Fau et al.[19, 20], concludes that $N_5^+N_5^-$ is a stable compound with high density (1.9 g/cm^3). They conclude that its performance as a rocket propellant is about the same as that of hydrazine but that its high density (about twice that of hydrazine) will allow for smaller and lighter rockets.

The second publication, by Evangelisti et al. [21], concludes that $N_5^+N_5^-$ is stable and that $(N_5^+N_5^-)_2$ is even more stable. They also conclude that the dimer stability suggests the possibility of a $N_5^+N_5^-$ crystal. Worth noticing here is that even though no crystal structure is calculated, calculations indicate that $(N_5^+N_5^-)_2$ has a planar, layered structure. This is very interesting since it is believed that such structures give less sensitive energetic materials[22].

The third publication, by Dixon et al. [23], concludes that both $N_5^+N_5^-$ and $N_5^+N_3^-$ are unstable. They have also experimentally confirmed that $N_5^+N_3^-$ really is unstable. Interestingly enough, despite their negative results, they state that “a hypothetical polynitrogen compound, such as $N_5^+N_5^-$, would be an excellent monopropellant for rocket propulsion or explosives, if it could be synthesized in a stable form”.

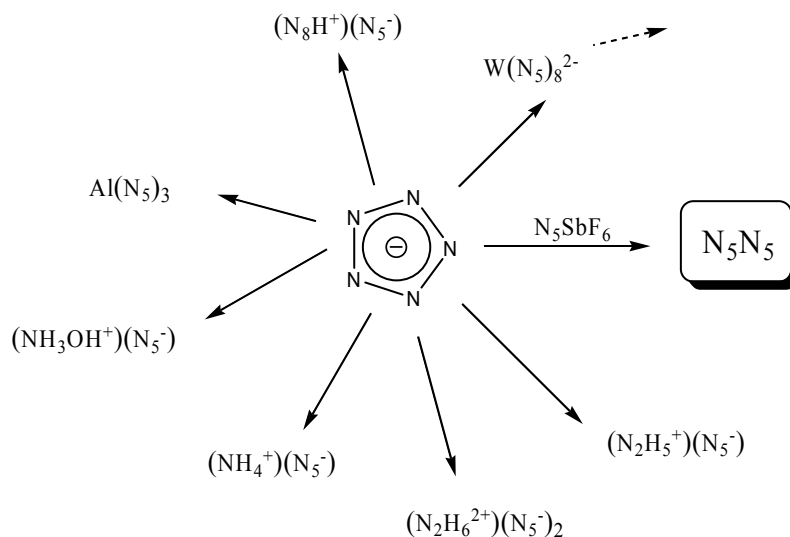
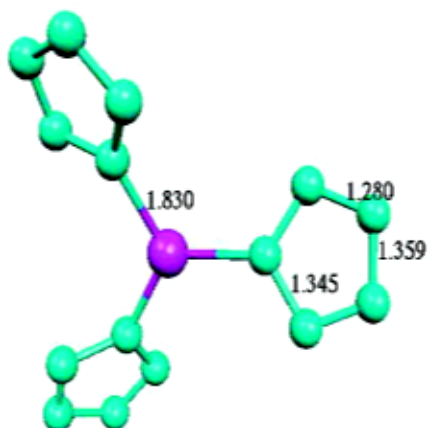


Figure 3 Once a stable complex with N_5^- has been made an ion exchange can be attempted in order to find a suitable counter ion.



7

Figure 4 *Computed structure of $Al(N_5)_3$ (from Straka[13]).*

In a recent quantum chemical study[13] some very interesting metal complexes with very high nitrogen content have been studied. Some of these complexes are charged and will need counter ions and some, such as $Al(N_5)_3$ (Figure 4), are neutral. The calculated heat of formation for these complexes is high although some are probably only marginally stable (Table 3). The high amount of nitrogen and the presence of heavy metal atoms gives a reasonable chance that they have high densities and therefore are interesting as HEDM's.

Table 3 *Calculated heat of formation for a few metal pentazolate complexes[13].*

Species	ΔH kJ/mol
$Al(N_5)_3$	1011
$Al(N_5)_4^-$	966
$Al(N_5)_6^{3-}$	1159
$Cr(N_5)_8^{2-}$	3536
$Mo(N_5)_8^{2-}$	3175
$W(N_5)_8^{2-}$	3167

4 Starting materials

The existence of arylpentazoles was proved without isolation of the substances[8, 24-26]. The kinetics of decomposition of various arylpentazoles has been investigated[24-27] as well as mechanisms of their formation[8, 24-28]. Arylpentazoles are difficult to isolate due to their low decomposition temperatures and only a few[27, 29] have been isolated successfully so far. The nitrogen ring structure of arylpentazoles has been proven by ^{15}N -labelling and measurement of molecular weight[30], ^{15}N -NMR spectroscopy[31] and X-ray analysis[32].

We have studied the stability of arylpentazoles theoretically and the results were published recently[33]. We have also synthesized and isolated many arylpentazoles in the lab. Our results on synthesis and stability of arylpentazoles are summarized in this chapter.

4.1 Synthesis of various starting materials

So far, the most stable pentazole made is *p*-dimethylaminophenylpentazole. It is however desirable to find other, possibly less stable, starting materials and a way to handle them safely and keep them until they can be studied. *p*-dimethylaminophenylpentazole is planar with strongly conjugated rings. This means that the bond that is subsequently to be broken is a very strong bond. It is therefore desirable to make a phenylpentazole in which this conjugation is broken but the pentazole ring is as stable as possible. A problem is of course that the conjugation is what stabilises the whole molecule which is sensitive enough *with* conjugated rings.

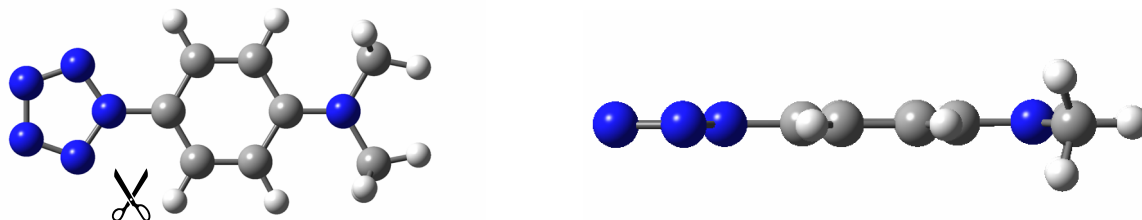


Figure 5 The bond between the N_5 ring and the phenyl ring needs to be broken in order to form N_5^- . *p*-dimethylaminophenylpentazole is planar with strongly conjugated rings leading to a very strong bond between the rings.

One way to break the conjugation would be to add groups that will force the rings out of plane. The attempted synthesis of the *o*-tertbutylphenyl- and 2,4,6-tri-tertbutylphenylpentazoles (Figure 6) has so far been unsuccessful, i.e. the products did not precipitate out of the reaction mixture or were not identified as pentazoles. However, the corresponding azides have been found which indicates that the azide has in fact reacted with the diazonium ion. Further investigation of this reaction is necessary to rule out the possibility that the pentazole is in fact formed in the reaction but decomposing too fast to allow successful detection. A possibility is to use ^{15}N labelled LiN_3 or NaNO_2 .

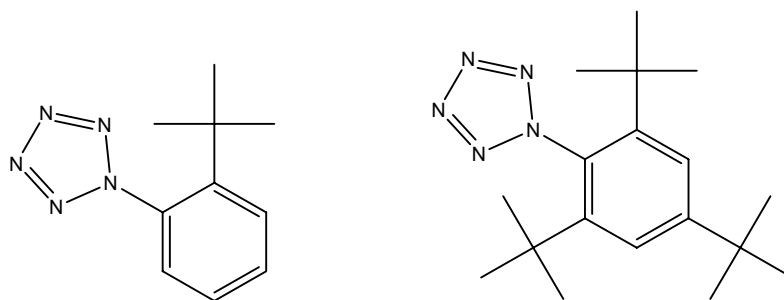


Figure 6 *The attempted synthesis of *o*-tertbutylphenylpentazole and 1,4,6-tri-tertbutylpentazole have not yet been successful.*

For arylpentazoles, it is desirable to have an electron donating group as substituent (see Figure 7) so that the electrons are pushed towards the N_5 ring. One such molecule is 4-pentazol-1-yl-phenol which was successfully used by Christie and co-workers to synthesise pentazolate in a mass spectrometer.

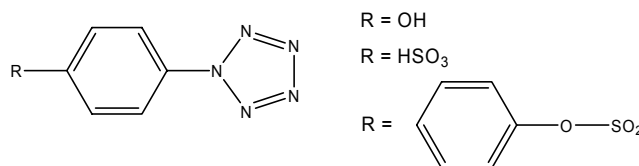
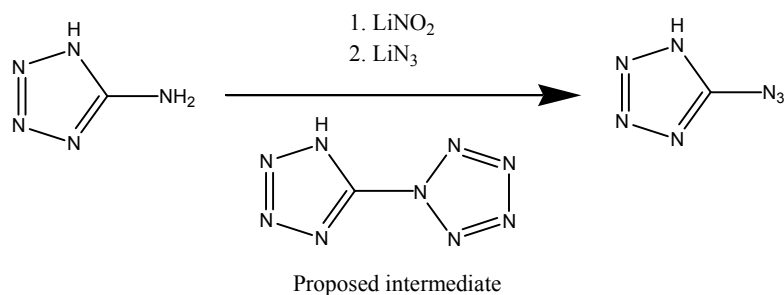
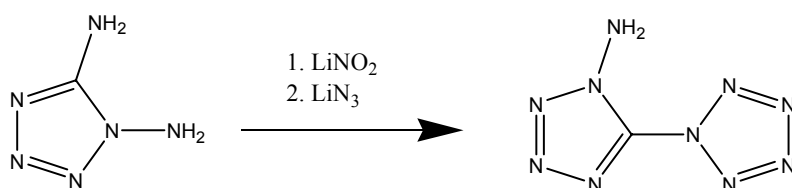


Figure 7 *The substituent, R, should be an electron donating group.*

Another possibility would be to use tetrazolpentazoles. There would be less conjugation between the tetrazole and pentazole rings. 1*H*-tetrazolylpentazole, the intermediate in Scheme 1, has been observed in a work by Hammerl and Klapötke [34]. This pentazole could not be isolated at the temperature and with the solvents used in these experiments but observations with ^{15}N -NMR spectroscopy strongly indicates that it is an intermediate in the reaction. In order to stabilise the pentazole ring an electron donating group such as NH_2 could be added to the tetrazole (Scheme 2).



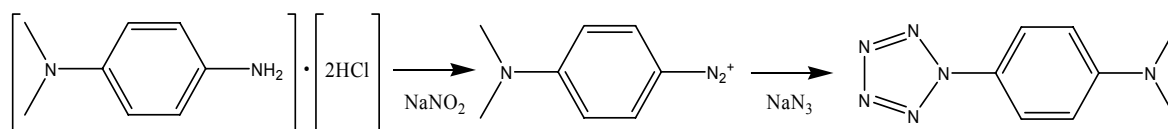
Scheme 1 Synthesis of 1H-tetrazolylpentazole



Scheme 2 Synthesis of 1-amino-tetrazolylpentazole

4.1.1 Synthesis of *p*-dimethylaminophenylpentazole

Unlabeled and ^{15}N mono- and dilabeled *p*-dimethylaminophenylpentazoles were synthesized as described below. The substances were kept under liquid N_2 . The samples were weighed in pre-cooled bottles. NMR samples were prepared by dissolving the substances in slightly cooled solvents and then cooling immediately to -20°C .



Scheme 3 Synthesis route to *p*-dimethylaminophenylpentazole.

***p*-dimethylaminophenylpentazole.** N,N -dimethylphenylenediamine dihydrochloride (3.137 g, 15.0 mmol) was dissolved in water (21 ml, cooled to 0°C). HCl (0.25 ml, 3.0 mmol) was then added. Under N_2 flow, solid NaNO_2 (1.138 g, 16.5 mmol) was added during 15 min, keeping the temperature of the reaction between -2 and 0°C . The reaction mixture was then stirred at the same temperature for 35 min. The reaction mixture was then transferred by syringe under N_2 flow to a mixture of MeOH (21 ml) and *n*-hexane (8 ml) cooled to -35°C by

an acetone-liquid N₂ bath. A saturated solution of NaN₃ (1.072 g, 16.5 mmol) in aqueous MeOH (15 mL, 50%) was added over several minutes. The reaction was stirred vigorously at -60°C for 40 min. The precipitated deep green-grey product was diluted with cold (-40°C) methanol (10 ml). All glass (including filters) and solutions, used in the following work were cooled to between -60 and -50°C by a cold bath of liquid N₂. The reaction suspension was filtered (f. 4). After the filtration, the filtrate was cooled by a cold bath to yield a second precipitate. While the 1-st precipitate was kept on filter in liquid N₂, the secondary precipitate was filtered (f. 4) off and washed with MeOH (2x10-15 mL), acetone (2x10 mL) and *n*-hexane (4 mL). The top of the filter was protected against water with foil. The filter was cooled using solid CO₂ and the precipitate dried by a water pump for 30-40 min to yield pure *p*-dimethylaminophenylpentazole (445 mg) as a shiny grey solid (from ¹H NMR in CD₂Cl₂ at -20°C). The same procedure was used to purify and dry the first precipitate resulting in 385 mg of grey-green *p*-dimethylaminophenylpentazole containing 10% of *p*-dimethylaminophenylazide (¹H NMR). The acetone washing solution contained almost pure *p*-dimethylaminophenylazide.

¹H NMR was carried out at -20°C in CD₂Cl₂ (5.35 ppm) or in CD₃CN (1.94 ppm). *p*-dimethylaminophenylpentazole: ¹H NMR (CD₂Cl₂) 7.96 (2H, d, *J*=9.1 Hz), 6.83 (2H, d, *J*=9.1 Hz), 3.10 (6H, s, Me); ¹³C NMR (CD₂Cl₂) 122.06 (d), 111.77 (d), 40.47 (q); *p*-dimethylaminophenylazide: ¹H NMR (CD₂Cl₂) 6.92 (2H, d, *J*=9.0 Hz), 6.77 (2H, d, *J*=9.0 Hz), 2.91 (6H, s, Me); ¹H NMR (CD₃CN) 6.94 (2H, d, *J*=9.0 Hz), 6.76 (2H, d, *J*=9.0 Hz), 2.96 (6H, s, Me); ¹³C NMR (CD₃CN) 149.76 (s), 128.87 (s), 120.71 (d), 114.83 (d), 41.04 (q). ¹³C NMR (CD₂Cl₂) 148.33 (s), 119.76 (d), 113.62 (d), 40.91 (q).

¹⁵N-dilabeled *p*-dimethylaminophenylpentazole. The same protocol as for unlabeled *p*-dimethylaminophenylpentazole was used, but in a slightly smaller scale. Only the differences are pointed out here. N,N-dimethylphenylenediamine dihydrochloride (1.248 g, 5.97 mmol) was dissolved in water (8 mL) and HCl (0.10 mL, 1.19 mmol) was added. Solid Na¹⁵NO₂ (460 mg, 6.57 mmol) was used. The reaction mixture was transferred to a mixture of MeOH (8 mL) and petroleum ether (1 mL). A saturated solution of Na¹⁵NNN (434 mg, 6.57 mmol) in aqueous MeOH (8 mL, 50%) was added. The first precipitate was washed with cold MeOH (3 mL), acetone (2 mL) and *n*-hexane (1 mL). After the drying as described above small amount of crude product (40 mg, mixture of *p*-dimethylaminophenylpentazole and *p*-dimethylaminophenylazide 1:0.5 according to ¹H NMR) was obtained. The cold filtrate was stirred for 15 min at -30°C and filtered again. The second precipitate was washed and dried as described above to get a product (65 mg, mixture 1:0.18) as grey solid. Then the

filtrate was kept stirring for 2.5 h between -20 and -25°C giving an additional third precipitate. The third precipitate was filtered, washed and dried using the same procedure giving 120 mg of grey solid as a mixture of *p*-dimethylaminophenylpentazole and *p*-dimethylaminophenylazide 1:0.15.

¹⁵N-monolabeled *p*-dimethylaminophenylpentazole. Na¹⁵NO₂ was used to produce ¹⁵N-monolabeled *p*-dimethylaminophenylpentazole. The same scale and the same protocol as for dilabeled *p*-dimethylaminophenylpentazole gave 310 mg product, containing 28% azide.

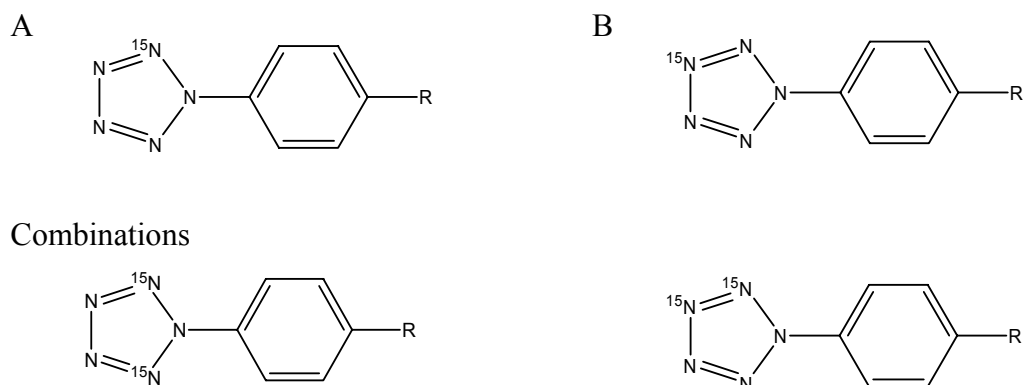


Figure 8 ¹⁵N-labelling of pentazoles.

4.1.2 Synthesis of *p*-methoxyphenylpentazole

***p*-methoxyphenylpentazole.** *p*-methoxyphenyl diazonium salt was obtained by the same method, as described above for synthesis of *p*-dimethylaminophenyl diazonium salt using an aqueous (22 mL) suspension of *p*-methoxyaniline (1.12 g, 9.2 mmol), conc. HCl (2.73 mL, 33.0 mmol) and NaNO₂ (0.69 g, 10.0 mmol). The solution of diazonium salt was added to a precooled (-40°C) mixture of *n*-hexane (88 mL) and methanol (12 mL). NaN₃ (1.30 g, 20 mmol) solution was added. After 15 min the reaction mixture was filtered, and the precipitate was washed with MeOH:H₂O 60:40 mixture (30 mL) and dried to get 550 mg of white powder as a mixture of *p*-methoxyphenylpentazole (Figure 9) and *p*-methoxyphenylazide 1:0.95. *p*-methoxyphenylpentazole: ¹H NMR (CD₃CN) 8.03 (2H, d, *J*=6.9), 7.17 (2H, d, *J*=6.9), 3.87 (3H, s); ¹³C NMR (CD₃CN) 162.46 (s), 123.60 (d), 115.64 (d), 55.80 (q). *p*-methoxyphenylazide: ¹H NMR (CD₃CN) 6.97 (2H, d, *J*=6.8), 6.91 (2H, d, *J*=6.8), 3.72 (3H, s); ¹³C NMR (CD₃CN) 158.18 (s), 133.19 (s), 121.04 (d), 116.20 (d).



Figure 9 *p*-methoxyphenylpentazole and *p*-tertbutylphenylpentazole

4.1.3 Synthesis of *p*-tertbutylphenylpentazole

***p*-tertbutylphenylpentazole.** *p*-tertbutylphenylpentazole (Figure 9) was obtained by the same protocol as *p*-methoxyphenylpentazole, starting from *p*-tertbutylphenylamine (2.38 mL, 15 mmol). Sodium nitrite (1.14 g, 16.5 mmol) and sodium azide (1.07 g, 16.5 mmol) were used for reaction. The reaction with sodium azide was completed in 20 min. The product was obtained as 1.45 g of unstable slightly pinkish powder as a mixture with azide 1:0.4. *p*-tertbutylphenylpentazole: ¹H NMR (CD₂Cl₂) 8.08 (2H, d), 7.67 (2H, d), 1.38 (9H, s, *t*-Bu). ¹³C NMR (CD₂Cl₂) 120.55 (d), 118.55 (d), 30.99 (q). *p*-tertbutylphenylazide: ¹H NMR (CD₂Cl₂) 7.41 (2H, d), 6.99 (2H, d), 1.33 (9H, s, *t*-Bu); ¹³C NMR (CD₂Cl₂) 148.75 (s), 137.64 (s), 127.29 (d), 119.08 (d), 34.68 (s), 31.62 (q).

To our knowledge this is the first time that *p*-tertbutylphenylpentazole has been synthesized.

4.1.4 Synthesis of *p*-nitrophenylpentazole

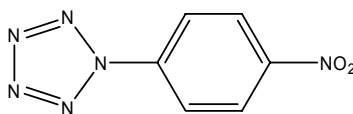
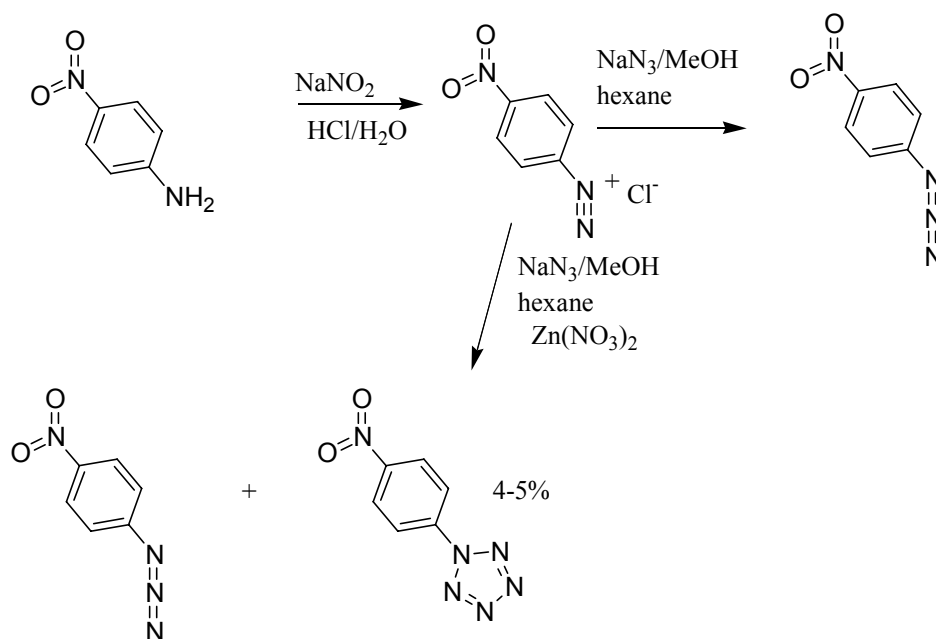


Figure 10 *p*-nitrophenylpentazole.

***p*-nitrophenylpentazole.** First, an attempt was made to get *p*-nitrophenylpentazole by the same procedure, as described above for the *p*-methoxy- derivative, but we were able to get only very pure light powder of *p*-nitrophenylazide, without any trace of the corresponding pentazole. The nitro group in para-position has very strong electron-withdrawing ability, and therefore causes the pentazole produced during the reaction to be extremely unstable. The

next attempt (Scheme 4) was made under the same reaction conditions, but NaN_3 addition to the mixture was followed by addition of 3 equivalents of $\text{Zn}(\text{NO}_3)_2$ in a minimum amount of water. After 30 min of stirring the solid was filtered off, washed with methanol:water 1:1 mixture (2x5 mL) and dried (work up at -32°C). According to ^1H NMR, the product is a mixture 1:0.04 *p*-nitrophenylazide : *p*-nitrophenylpentazole. Heating up the sample to 25°C caused immediate disappearance of pentazole signals. *p*-nitrophenylpentazole: ^1H NMR (CD_3CN) 8.51 (2H, d), 8.39 (2H, d). *p*-nitrophenylazide: ^1H NMR (CD_3CN) 8.22 (2H, d), 7.22 (2H, d). ^{13}C NMR (CD_3CN) 126.49 (d), 125.05 (s), 120.70 (d).



Scheme 4 Synthesis of *p*-nitrophenylpentazole.

4.1.5 Salts of *p*-pentazolephenylsulfonic acid

The synthesis of salts of *p*-pentazolephenylsulphonic acid turned out to be quite tricky. The NMR proton shifts for *p*-pentazolephenylsulphonic acid are easily confused with the shifts of the diazonium salt of *p*-phenylsulphonic acid. Even though the diazonium salt was not the desired product, it turned out to be remarkably stable and the synthesis route and some other information is given in the first section of this chapter.

4.1.5.1 A stable diazonium salt of *p*-pentazolephenylsulphonic acid

Diazonium salt of *p*-phenylsulphonic acid. To a suspension of sulfanilic acid (2.60 g, 15.0 mmol) in water (15 mL), 8 mL aqueous solution of Na₂CO₃ (0.883 g, 8.33 mmol) was added dropwise. After 10 min when everything was dissolved, the solution was cooled down to 15°C and NaNO₂ (1.14 g, 16.5 mmol) added to the solution in 10 min. After 10 min of stirring at the same temperature the reaction mixture was poured into crushed ice (17.0 g), containing conc. hydrochloric acid (3.60 mL, 43.5 mmol). After 15 min the resulting cold (0°C), thick white suspension of diazotated sulfanilic acid was added to the precooled (-40°C) and vigorously stirred suspension of BaCl₂ (7.32 g, 30.0 mmol) in water (15 mL) and methanol (65 mL). The reaction mixture was kept at the same temperature (-40°C) during reaction and work up. A saturated solution of NaN₃ (1.31 g, 18.6 mmol) in 60:40 mixture of methanol:water (16 mL), precooled to -20°C, was added dropwise in 10 min. Stirring was continued for the next two hours, before the produced, thick suspension was filtered through the filter with cooling jacket (-30°C) and carefully washed with cold (-40°C) 60:40 mixture methanol-water (2x15 mL) and acetone (10 mL) and dried at the same temperature to give the product (white powder, 3.05 g). The mother filtrate was kept overnight at room temperature. Fine white crystals precipitated during that time. The same work up as for the first product performed at room temperature gave the second portion of product (1.01 g).

The first product was found to be completely insoluble at -20°C in acetonitrile or methanol. It was dissolved at 25°C in DMSO-d₆. ¹H NMR discovered a mixture of signals, belonging to the diazonium salt of *p*-phenylsulphonic acid and *p*-azidephenylsulphonic acid, in a ratio of 1:0.5. Running ¹³C NMR at the same temperature (25°C) during 18 h showed insignificant degradation of the diazonium salt upon that period. One sample was dissolved in DMSO-d₆ at approximately 45-50°C. ¹H NMR at 25°C showed that it consisted of a mixture of diazonium salt, azide, and small amount of sulfanilic acid, though the diazonium salt was still a main component. According to proton NMR (DMSO-d₆ at 25°C) the second product was pure azide. This result has also been compared to the results of a recently published article[35].

The mixture of the diazonium salt and azide was purified by suspending in dimethylformamide (50 mg of mixture in 1 mL of DMF), filtering from the solvent, washing by several mL of DMF and drying at room temperature with protection from light. The substance was crystallized from ice-cold water to give white crystals. These crystals did not show any degradation even after several weeks at room temperature.

Due to the similarity between the proton shifts of *p*-pentazolephenylsulphonic acid and the diazonium salt of *p*-phenylsulphonic acid (between 8.0 and 8.6 ppm, which is highly typical for all arylpentazole) it was first believed that these crystals were the pentazole. However, X-ray analysis (Figure 11) of the substance showed that it is a zwitter diazonium salt of *p*-phenylsulphonic acid.

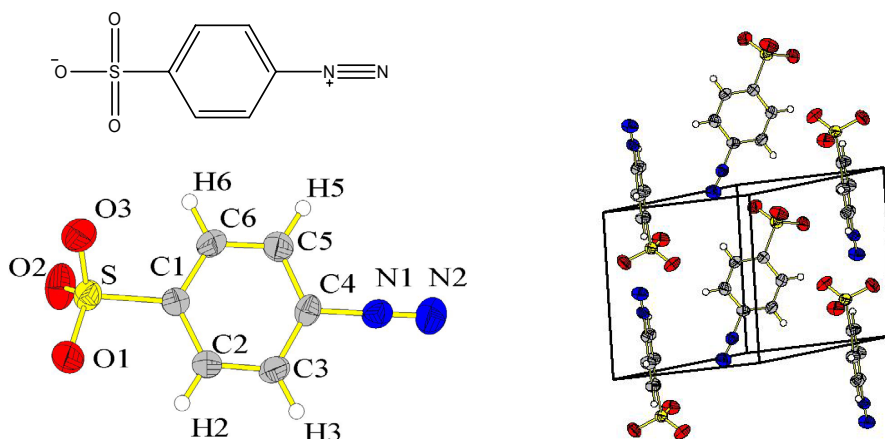


Figure 11 The structure of the substance believed to be the Barium salt of *p*-pentazolephenylsulphonic acid as determined by X-ray. It turned out to be *p*-diazophenylsulphonic acid.

This substance has remarkable stability: dynamic NMR in D₂O at 25°C still had over 10% of starting material after 13 days, in DMSO-d₆ – after 9 days. The substance could be stored at room temperature under light protection without any decomposition. Generally, phenyldiazonium salts are very unstable and reactive compounds.

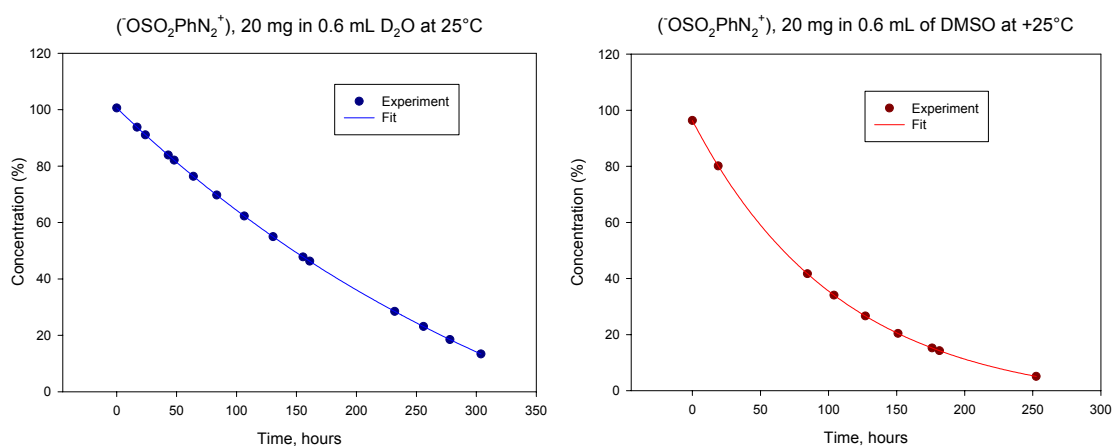
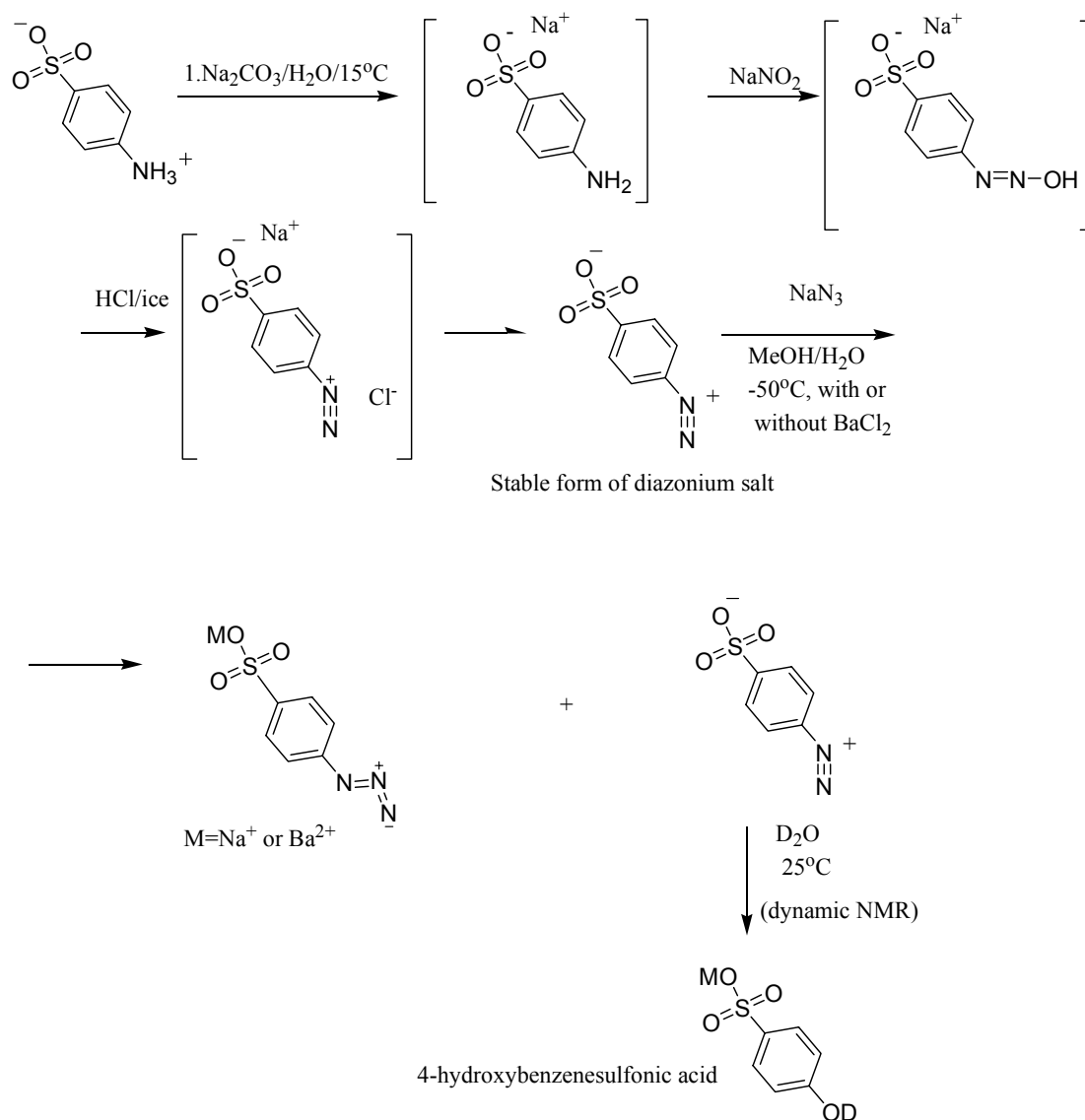


Figure 12 Dynamic NMR measurements of *p*-diazophenylsulphonic acid.

Later we isolated the diazonium salt of *p*-phenylsulfonic acid directly after the diazotation, to have an authentic reference for NMR shifts and DSC pattern, but already after 15 h at room temperature the salt was partly destroyed. The single product of its degradation under dynamic NMR conditions must be *p*-hydroxybenzenesulfonic acid.

We can suggest that that remarkable stability of diazonium salt of *p*-phenylsulfonic acid, isolated from the reaction, was caused by a stabilizing effect of BaCl_2 . The presence of barium was not found in the X-ray analysis but barium was detected by precipitation of BaSO_4 from a water solution upon adding sulphuric acid.



Scheme 5 First attempt to synthesise the barium salt of *p*-pentazolephenylsulfonic acid resulting in the diazonium salt

4.1.5.2 Sodium, potassium and barium salts of *p*-pentazolephenylsulfonic acid

In a new experiment, the diazonium salt was isolated and dried from water and in the next step reacted with sodium azide in dry methanol. In detail this means that the diazonium salt of sulfanilic acid was obtained as described on page 24, starting from sulfanilic acid (2.60 g, 15.0 mmol) After 15 min of stirring the resulting cold (0°C) thick white suspension of diazotated sulfanilic acid was quickly filtered, washed with 2x5 mL ice-cold water, dried on filter by vacuo during 10 min and suspended in precooled to -20°C dry methanol (35 mL). The suspension was cooled to -50°C before the saturated solution of NaN₃ (975 mg, 15 mmol) in dry methanol (30 mL), precooled to -50°C, was added dropwise to the reaction in 30 min. Stirring was continued for the next 4.5 hours at the same temperature, until the precipitation disappeared and a lightly coloured solution was produced. An NMR sample, taken from reaction mixture, and carried out in CD₃OD at -20°C showed an absence of diazonium salt signals, though two sets of signals, belonging to Na⁺(⁻OSO₂PhN₅)[35] and Na⁺(⁻OSO₂PhN₃) in a ratio 1:4. In order to get the product as a solid, a suspension of Ba(OH)₂•H₂O (789 mg, 2.5 mmol) in dry methanol (20 mL), precooled to -50°C was added to the solution during 5 min. After 2.5 hours of stirring at -50°C, the produced suspension was filtered through a filter with cooling jacket (-30°C), and washed with 2x5 mL of cold (-50°C) dry methanol, and dried on the same filter at the same (-30°C) temperature to give the product (white powder, 1.24 g). ¹H NMR (in CD₃OD at -20°C) shows two sets of signals, supposedly belonging to Ba²⁺(⁻OSO₂PhN₅)₂ and Ba²⁺(⁻OSO₂PhN₃)₂ in ratio 1:1.9. Using KOH (0.35 eq) gave identical results with nearly exactly the same ratio of K⁺(⁻OSO₂PhN₅) and K⁺(⁻OSO₂PhN₃). In the NMR sample from the mother filtrate, kept at -40°C only small amounts of arylazide were discovered. Barium or potassium salts of *p*-pentazolphenylsulfonate did not demonstrate any special difference in stability, and after 5 min at +10°C they degraded totally to the azides.

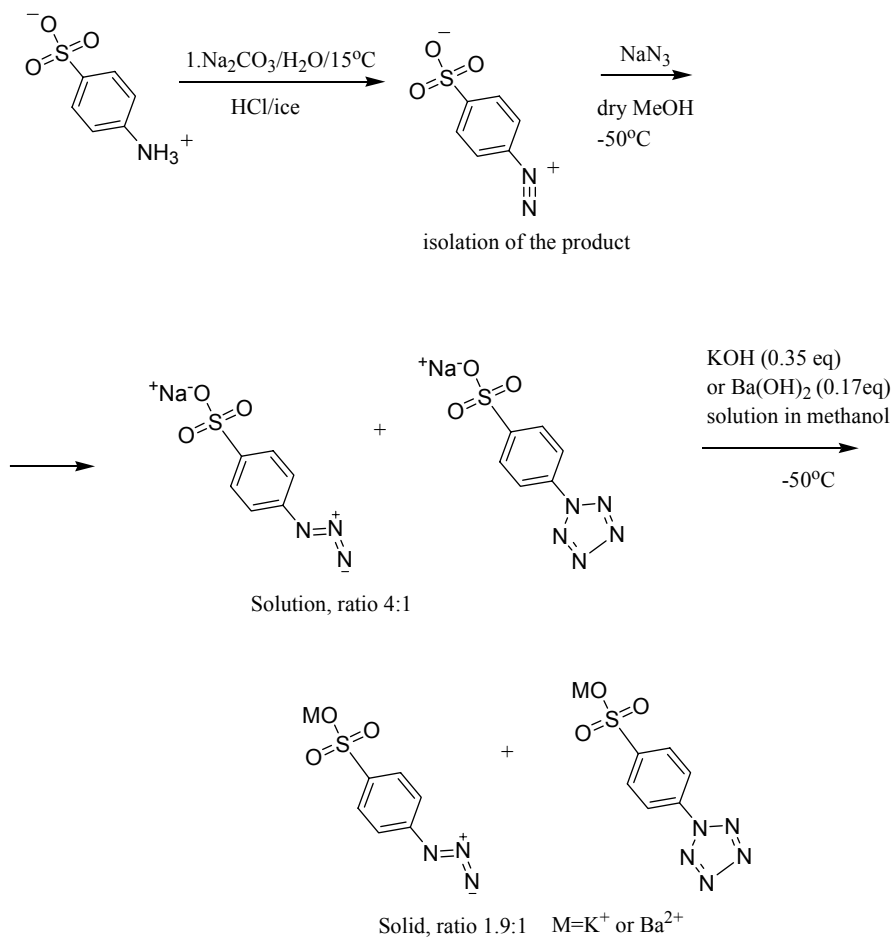
Chemical shifts of sodium, potassium or barium salts of pentazole or azide respectively are the same. Different solvents changes some of the shifts of the NMR signals.

Diazonium salt of p-phenylsulfonic acid: ¹H NMR (CD₃CN) 8.65 (2H, d, *J*=8.9), 8.10 (2H, d, *J*=8.9); ¹H NMR (DMSO) 8.66 (2H, d, *J*=8.9), 8.10 (2H, d, *J*=8.9); ¹³C NMR (DMSO-d₆) 144.10 (s), 142.30 (s), 133.32 (d), 127.95 (d). ¹H NMR (D₂O) 8.73 (2H, d, *J*=8.9), 8.31 (2H, d, *J*=8.9). ¹H NMR (CD₃OD) 8.69 (2H, d, *J*=8.0), 8.29 (2H, d, *J*=8.0).

Barium (potassium, sodium) p-pentazolephenylsulfonate: ¹H NMR (CD₃OD) 8.35 (2H, d, *J*=8.8), 8.15 (2H, d, *J*=8.8). ¹³C NMR (CD₃OD) 148.8 (s), 136.2 (s), 129.2 (d), 122.4 (d).

Barium (potassium, sodium) p-azidophenylsulfonate: ^1H NMR (D_2O) 7.78 (2H, d, $J=7.5$), 7.19 (2H, $J=7.5$). ^{13}C NMR (D_2O) 143.48 (s), 138.90 (s), 127.55 (d), 119.61 (d). ^1H NMR (CD_3CN) 7.61 (2H, d), 7.06 (2H, d). ^{13}C NMR (CD_3CN) 145.44 (s), 139.24 (s), 127.35 (d), 118.27 (d). ^1H NMR (CD_3OD) 7.84 (2H, d, $J=7.8$), 7.17 (2H, $J=7.8$).

p-Hydroxyphenylsulfonic acid: ^1H NMR (D_2O) 7.65 (2H, d, $J=7.9$), 6.93 (2H, d, $J=7.9$).



Scheme 6 Synthesis of sodium, potassium and barium salts of *p*-pentazolephenylsulfonic acid.

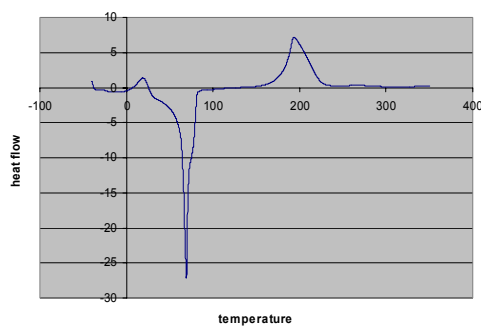
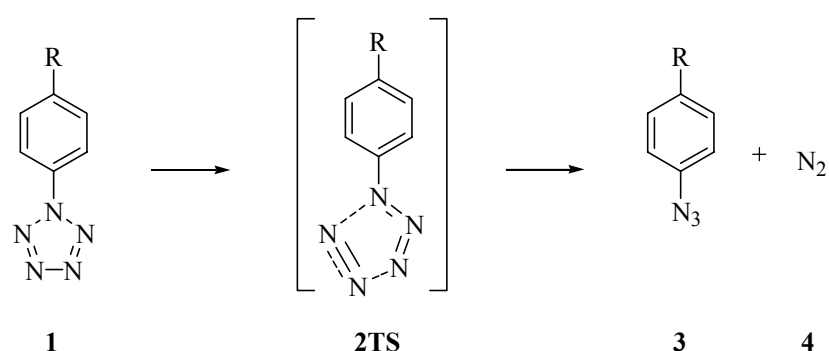


Figure 13 DSC spectrum of a mixture of the potassium salts of *p*-pentazolephenylsulfonic acid and *p*-azidophenylsulfonic acids in a ratio 0.53:1.

4.2 The stability of arylpentazoles, QM calculations

The stability of different para substituted arylpentazoles has previously been studied both experimentally and theoretically [24, 27, 29]. We have studied several arylpentazoles computationally with added solvent effects corresponding to the polar solvent methanol. This was done to establish the effect of different substituents on the decomposition rate. All optimizations were performed at the DFT-B3LYP/6-31+G(d) level of theory and energies were evaluated at the DFT-B3LYP/6-311+G(2df,p) level (Scheme 7).



Scheme 7 The decomposition of arylpentazole, *R* = *H*, NH₂, NO₂...

4.2.1 Calculated activation energies

The results from the calculations for the decomposition of the arylpentazoles are presented in Table 4. The computed solvent effects confirm that the stability of the para substituted arylpentazoles increases in polar solvents[27]. The stabilization is believed to be a consequence of the ground state being of more polar character than the transition state[29]. The different evaluated compounds also confirm that the stability of arylpentazoles increase with electron donating groups (e.g. NH₂) and decreases with electron withdrawing groups (e.g. NO₂). As reported in other studies[24, 29] the arylpentazole with O⁻ as substituent was found to be the most stable of the para-substituted compounds. The calculated stability of the different arylpentazoles agrees well with experimental values.

Table 4 Activation energies (B3LYP/6-311+G(2df,2p)) for the decomposition of arylpentazole. All energies are presented in kcal/mol ^a.

-R	ΔE^\ddagger	ΔG_g^{\ddagger}	$\Delta\Delta G_{PCM}$	$\Delta G_{sol}^{\ddagger}$	$\Delta G_{sol, Exp}^{\ddagger}$ ^b
-NO ₂	18.6	15.2	2.7	17.9	18.7
-HSO ₃	18.8	15.4	2.9	18.3	-
-CN	19.0	15.5	3.0	18.5	-
-N ₅	19.1	15.3	3.1	18.4	-
-CF ₃	19.3	15.8	3.1	18.9	-
-H	20.2	16.5	3.0	19.5	19.8
-Cl	20.1	17.4	3.1	20.5	19.6
-CH ₃	20.7	17.7	3.1	20.8	20.0
-OH	20.9	17.7	3.1	20.8	20.3
-NH ₂	21.3	18.1	3.0	21.1	-
-N(CH ₃) ₂	21.5	18.3	3.0	21.3	20.7
-SO ₃ ⁻	22.6	21.5	1.4	22.9	-
-O ⁻	24.0	20.8	1.2	22.0	21.0

^a The definitions for the energetics (with respect to the reactants) are $\Delta G_g^{\ddagger} = \Delta E + \Delta\Delta G_g$, $\Delta\Delta G_g$, is the free energy correction calculated at 273.15 K; $\Delta\Delta G_{PCM}$: PCM solvation free energy correction, methanol.

^b Experimental values are estimated from reaction rates in methanol at 273.15 K.[24]

4.2.2 Effect of the TS structure on stability

When studying the transition state structure for the different para-substituted arylpentazoles an interesting fact becomes evident. The unsubstituted arylpentazole, phenylpentazole, has a TS-structure which is rotated out of plane. This rotation is increased for arylpentazoles with electron-donating groups, or rather resonance-donating groups such as -NH₂ and -OH. The TS-structures for arylpentazoles with electron-withdrawing groups are in plane. This difference between the two groups of arylpentazoles leads to the conclusion that the stability of arylpentazoles is due to resonance over the two rings. The *cyclo*-N₅⁻ ion is known to owe its stability to aromatic resonance stabilization. This also seems to hold for arylpentazoles. The pentazole moiety is stabilized by resonance which must be broken for it to decompose. Substituents such as chloride, trifluoromethyl, and methyl are interesting to discuss since they represent special cases. *p*-chlorophenylpentazole should be less stable than

phenylpentazole if one should only consider chloride's electron-withdrawing capacity. However, since chloride is resonance-donating the resonance stabilization is not disturbed and the stability is equal to that for unsubstituted arylpentazole. The electron-withdrawing effect of trifluoromethyl seem to be enough to disturb the resonance over the two rings, the TS-structure is planar and the activation energy lower than for phenylpentazole. Finally, methyl, an electron-donating substituent with no resonance-donating ability has a rotated TS-structure and a decreased decomposition rate. The conclusion should be that electron-donating groups stabilize arylpentazoles but groups that are also resonance-donating have a larger effect on the stability and the reverse being true for electron- and resonance-withdrawing groups.

4.2.3 Ortho substituted *p*-aminophenylpentazole

Following the reasoning above one way to increase the stability of arylpentazoles would be to add groups which would prevent or at least hinder the breaking of resonance. A well known procedure for this is to introduce internal hydrogen bonds. Two substituted arylpentazoles were studied for this purpose. The 2-hydroxyl-4-aminophenylpentazole has one internal hydrogen bond from the hydroxyl proton to the N₂ atom of the pentazole ring. Calculations showed an activation energy of 22.6 kcal/mol (Table 5), which is an increase in stability by 1.3 kcal/mol compared to *p*-aminophenylpentazole. The introduction of a second internal hydrogen bond (2,6-dihydroxy-4-aminophenylpentazole) increase the stability further (23.9 kcal/mol). These calculations show the importance of resonance and also predict 2,6-dihydroxy-4-aminophenylpentazole to be the most stable non-charged arylpentazole in solid/gas-phase in this theoretical study. The introduction of bulky groups ortho to the pentazole group should lead to a steric hindrance of resonance and hence very unstable compounds. The calculations of 2-methyl-4-aminophenylpentazole and 2-oxy-4-aminophenylpentazole anion show a decrease in stability, -1.7 and -1.4 kcal/mol, respectively relative *p*-aminophenylpentazole. A further indication for the importance of resonance for the stability of arylpentazole is that the free energy relationship correlates better with σ^+ than with σ_p , $R^2=0.9552$ and 0.9372 respectively.

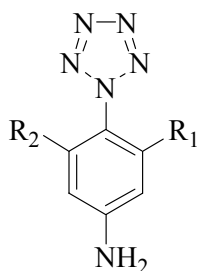


Figure 14 *Ortho-substituted p-aminophenylpentazole.*

Table 5 *Activation energies (B3LYP/6-31+G*) for the decomposition of ortho-substituted p-aminophenylpentazole (Figure 14). All energies are presented in kcal/mol^a.*

-R ₁	-R ₂	$\Delta E_{\ddagger}^{\ddagger}$	$\Delta G_{g}^{\circ\ddagger}$	$\Delta\Delta G_{PCM}$	$\Delta G^{\circ\ddagger}_{sol}$
-OH	-OH	23.9	19.1	-0.5	18.6
-OH	-H	22.6	19.0	1.1	20.1
-CH ₃	-H	19.6	16.3	2.8	19.1
-O-	-H	19.9	17.3	2.2	19.5

^a See Table 4

To investigate the electron-withdrawing effect of the pentazole ring the activation energy for arylpentazole with *cyclo*-N₅ as the *p*-substituent was calculated. Through the free energy relationship σ_p was estimated to 0.45 and σ^+ was estimated to 0.80. This shows that the pentazole ring has a similar inductive electron-drawing effect as -NO₂.

4.2.4 Implications for the benzyne mechanism

In evaluating the stability of arylpentazoles it was found that resonance-donating groups increase their lifetime. In the benzyne mechanism (discussed in chapter 6) a negative intermediate (Figure 15) is formed rather easily by abstraction of the ortho-proton from phenylpentazole. This intermediate, with a free electron pair, should be very stable due to the strong electron donating ability of the free electron pair.

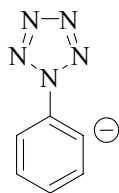


Figure 15 *The intermediate in the benzyne reaction.*

The free energy of activation for the decomposition of the intermediate at 298 K was found to be 21.9 kcal/mol, which is in the same order as the most stable mono-substituted arylpentazole (4-oxophenylpentazole anion).

4.2.5 The stability of tetrazolpentazoles

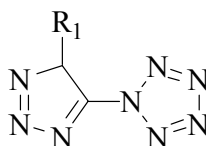


Figure 16 *Tetrazolpentazoles, $R_1 = H, NH_2$*

A further possibility is to use tetrazolpentazoles (Figure 16) as a source for the pentazolate anion; the tetrazolpentazolate should be less conjugated. 1H-tetrazolylpentazole has been observed in work done by Hammerl and Klapötke[34]. The intermediate has not been isolated but ^{15}N -NMR spectroscopy indicates that it is in fact present. In order to stabilize the intermediate for isolation an electron-donating group such as NH_2 could be added to the tetrazole, this has been investigated at the B3LYP/6-31+G(d) level of theory (Table 6).

Table 6 *Activation energies (B3LYP/6-31+G*) for the decomposition of 1H- and 1NH₂-tetrazolylpentazole. All energies are presented in kcal/mol^a.*

-R1	ΔE^\ddagger	$\Delta G^{\circ\ddagger}$	$\Delta\Delta\text{GPCM}$	$\Delta G^{\circ\ddagger}\text{sol}$
-NH ₂	16.1	13.3	2.1	15.5
-H	16.7	14.3	1.4	15.7

^a See Table 4

The results show that adding an electron-donating group does not increase the stability of the tetrazolypentazole, the stability is instead decreased. This is due to the increased stability of the formed azide. The degradation of 1NH₂-tetrazolypentazole leads to a more stable azide than the decomposition of 1H-tetrazolypentazole; i.e. the reaction is more exergonic by 4.8 kcal/mol.

5 Detection

There are a few possible methods that may be suitable for detection of N_5^- . These are Raman spectroscopy, IR spectroscopy, Coherent Anti-stokes Raman Scattering (CARS), NMR spectroscopy and Mass spectrometry. The basics of these methods as well as some theoretical and experimental results, when applicable, are presented in this chapter.

5.1 Raman and IR absorption spectroscopy

The principles for Raman Spectroscopy are described in for example many textbooks on lasers and spectroscopy[36]. A laser with frequency ω_L (Figure 17) is used to excite the molecules to a virtual level of the molecule. The molecule then emits Raman Scattered light of a higher (Stokes radiation) or a lower (Anti-Stokes radiation) frequency ω_S/ω_A . If the molecule that scatters the light is in its ground state, then the energy level to which it is deexcited is for example a higher vibrational state.

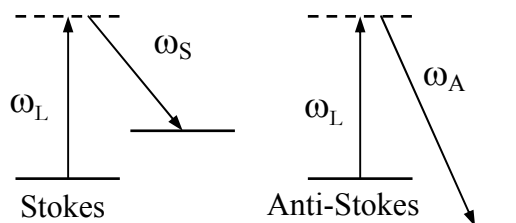


Figure 17 Schematic level diagram of Raman Spectroscopy

Table 7 Calculated vibrational frequencies of cyclo- N_5^- .

N_5^- (D_{5h})	IR int.	Raman int.	Raman depolarisation ratio	Vibrational frequency (cm^{-1})
E_2''	0.0	0.0	0.75	782.7
E_2'	0.0	3.6	0.75	1059.5
E_2'	0.0	2.0	0.75	1124.2
A_1'	0.0	47.8	0.04	1222.4
E_1'	27.2	0.0	0.75	1286.1

Calculated vibrational frequencies according to Perera and Bartlett[37] are shown in Table 7. As can be seen from the table, there are three Raman lines, one strong and two weaker, as well as one weak IR line. The fact that there is only one IR line is due to the high symmetry of the molecule and the fact that it therefore does not have a permanent dipole moment. A combination of Raman and IR lines for detection of N_5^- can be used.

5.2 CARS – Coherent Anti-Stokes Raman Scattering

A general difficulty using Raman spectroscopy and in this case also IR absorption is the weak nature of the process. The detection limit of N_4 , which has a calculated Raman intensity of the same order of magnitude as N_5^- , in a nitrogen matrix has been estimated[38] in our lab before. A combination of calculations and experiment, comparing the calculated Raman intensity of N_4 (which has not been made so that it cannot be measured) with that of N_2 , which can be easily measured, gives a detection limit of 80 ppm. IR absorption is normally a much stronger process but due to the total symmetry of the pentazole anion and the subsequent lack of dipole moment the one IR line is also a very weak one although not impossible to find.

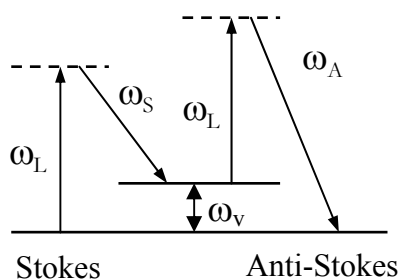


Figure 18 Schematic level diagram of Coherent Anti-Stokes Raman Spectroscopy (CARS)

Coherent Anti-Stokes Raman Spectroscopy (CARS) is a technique to take advantage of non-linear effects of Raman scattering. Descriptions of the theory can be found in for example textbooks on lasers and Raman spectroscopy[36]. Two lasers with frequencies ω_1 and ω_2 (Figure 18), where $\omega_1 - \omega_2 = \omega_v$ and ω_v is the frequency of a Raman active vibration in the studied molecule, are used. Provided that correct phase matching is obtained anti-Stokes radiation with frequency $\omega_A = 2\omega_1 - \omega_2$ and Stokes radiation with frequency $\omega_S = 2\omega_2 - \omega_1$ are

generated. The advantages of CARS are high signal strengths due to non-linear effects as well as the well-defined direction of the signal. In gases the phase-matching condition can normally be met with collinear beams in which case the Stokes and anti-Stokes radiation is generated in the same direction as the incident laser beams. The dispersion effects in liquids normally cause the phase-matching condition to be met only with crossed beams.

5.3 NMR spectroscopy

NMR spectroscopy can be used to study pentazoles in solutions. Rather than using ^{15}N -NMR spectroscopy which gives weak signals and requires hours of recording to get a good spectrum, ^1H -NMR has been used. The NMR shifts of the carbon attached to the pentazole ring and the protons on the carbons next to it (Figure 19) can be used as the shifts are clearly different in the azide compared to the pentazole[39]. By following the ratio between the azide and pentazole signals with time, the decomposition rate can be determined.

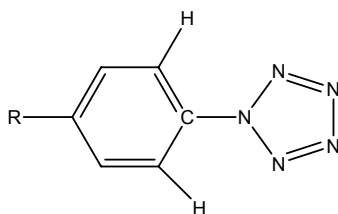


Figure 19 ^1H -NMR has been used to study the decomposition of pentazoles. The carbon atom and the protons that can be used are written out for clarity.

5.3.1 Reaction kinetics measurements with ^1H -NMR

The decomposition of pentazoles into the corresponding azides has been studied. The complexation between pentazoles and metal ions as described previously, can also be studied by this type of measurements. If a complexation in fact takes place this should influence the decomposition rate. So far only addition of lithium ions in the form of lithiumperchlorate has been tried using NMR techniques.

A number of dynamic proton NMR measurements were made on *p*-dimethylaminophenylpentazole to estimate the rate constant *k* of decomposition (Table 8) at different temperatures (0, +5, +10, +15, +25°C) (Figure 20) using different solvents (CD₂Cl₂, CD₃CN, CD₂Cl₂/CD₃OD mixture at +10°C) and with or without inorganic salt (LiClO₄). We have shown, that the decomposition rate of *p*-dimethylaminophenylpentazole is lower in acetonitrile, and higher in dichloromethane and methanol:dichloromethane 0.8:1 mixture. There was a slight decrease of *k* in the presence of lithium perchlorate the CD₂Cl₂:CD₃OD (Figure 21).

An attempt to run dynamic proton NMR of *p*-dimethylaminophenylpentazole to estimate the influence of presence CoCl₂ on stability of the pentazole at +10°C in CD₂Cl₂-CD₃OD. Unfortunately, cobalt together with ferrum and nickel belong to the group of the metals that interfere with NMR measurements, resulting in strong broadening of all signals. In result, the measurement error was too high to trust the results. We are planning to run dynamic ¹H-NMR of *p*-dimethylaminophenylpentazole in the presence of BaCl₂ and Zn(NO₃)₂. Still, it is technically possible to run dynamic ¹³C NMR in the presence of a Co²⁺ salt.

Table 8 Decomposition rates of *p*-dimethylaminophenylpentazole measured by ¹H-NMR. The error in the last digit as indicated in parenthesis is the standard deviation of the fit.

Solvent	<i>T</i> (°C)	Metal ion	<i>C</i> (mM) ^a	<i>k</i> ·10 ⁴ s ⁻¹
CD ₂ Cl ₂	0	-	-	2.72(16)
CD ₂ Cl ₂	5	-	-	2.78(11)
CD ₂ Cl ₂	10	-	-	5.07(61)
CD ₂ Cl ₂	15	-	-	9.92(74)
CD ₂ Cl ₂	25	-	-	35(12)
CD ₃ CN	10	-	-	3.84(16)
CD ₃ CN	10	Li ⁺	150	3.80(16)
CD ₃ OD:CD ₂ Cl ₂ 0.8:1	10	-	-	5.31(22)
CD ₃ OD:CD ₂ Cl ₂ 0.8:1	10	Li ⁺	600	4.84(9)

^a the concentration is only given approximately

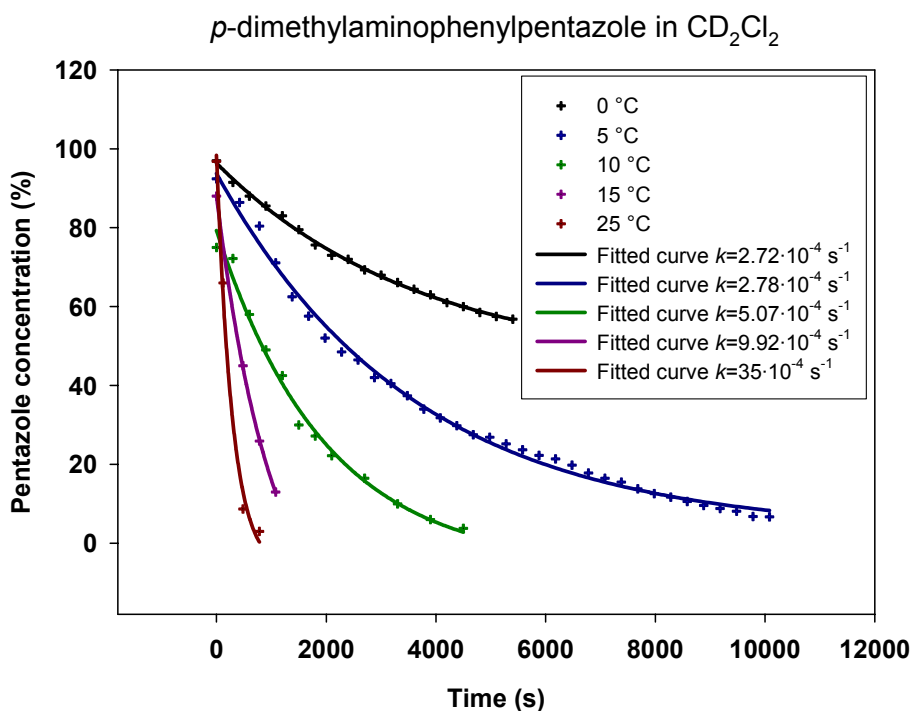


Figure 20 The *p*-dimethylaminophenylpentazole concentration in relation to *p*-dimethylaminophenylazide in CD₂Cl₂ solution at different temperatures as measured by ¹H-NMR.

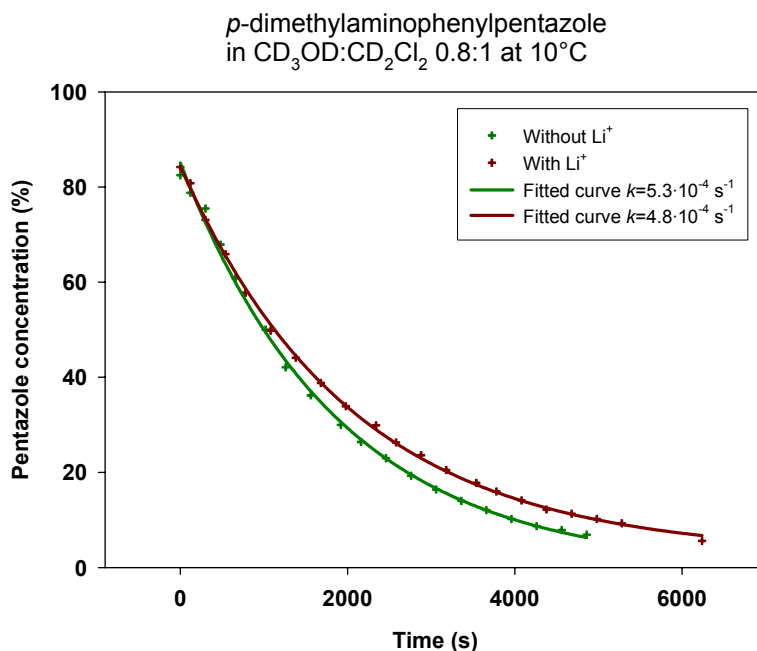


Figure 21 The *p*-dimethylaminophenylpentazole concentration in relation to *p*-dimethylaminophenylazide in a solution of CD₃OD:CD₂Cl₂ 0.8:1 at 10°C as measured by ¹H-NMR with and without LiClO₄.

The Arrhenius equation, $k = Ae^{-E_a/RT}$, has been used to determine the activation energy, E_a . The fit (Figure 22) gives $E_a=20.9$ kcal/mol.

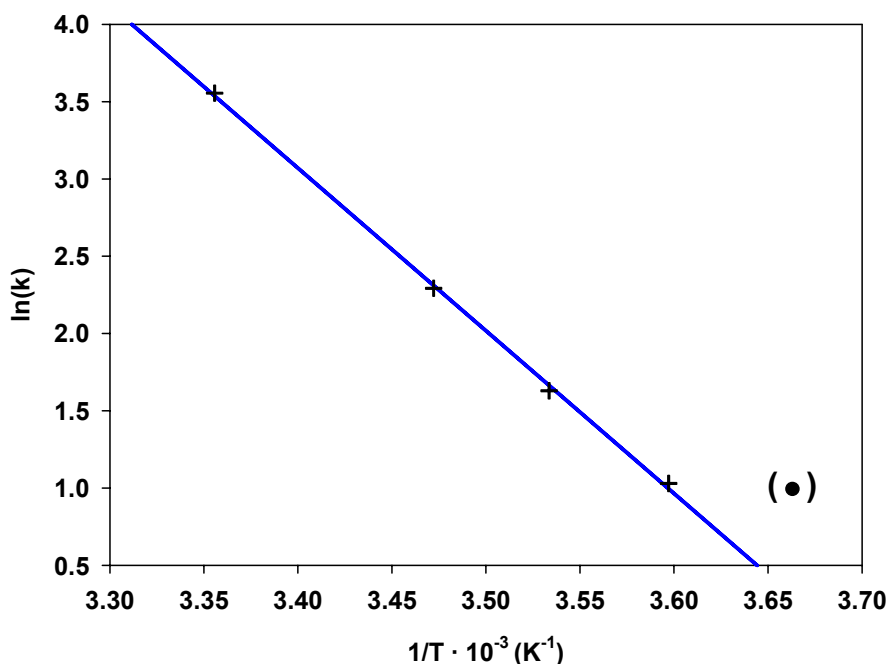


Figure 22 Arrhenius plot of *p*-dimethylaminophenylpentazole decomposition in CD_2Cl_2 . From this plot it is evident that there is a bad measurement at 0 °C. The error is most likely the temperature reading. This point has therefore been excluded in the fit.

5.3.2 ^{15}N - and ^{14}N -NMR, theoretical calculations

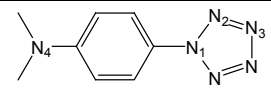
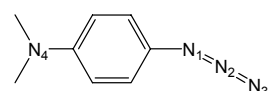
One problem with ^{15}N -NMR measurements are the very weak signals requiring long measurement times (days-weeks). ^{14}N -NMR measurements are faster to perform but the lines are normally much broader. However this should not prove a problem in our case since we have a well defined problem and only need to be able to distinguish between starting materials and reaction products. In Figure 23, a ^{14}N -NMR spectrum of 2,4-dichlorophenylpentazole is shown. It is clearly seen that by comparison with the calculated shifts the resolution is good enough to distinguish between the arylpentazole and the pentazolite ion and hereby provide an easier way of studying and detecting pentazolite ions in solution.

The synthesis of pentazoles may also be studied by allowing the reaction to take place inside the NMR. This way everything can easily be kept cold and it would be possible to see if some of the more unstable pentazoles form at all during the synthesis and just decompose

before they can be studied by other means. If they are forming at all it may be possible to find a way to break off the pentazole ring before decomposition to the azide.

Theoretical calculations of the NMR spectrum from pentazolate and *p*-dimethylaminophenylpentazole have been made. First, the geometry was optimised at B3LYP/6-31+G(d,p) level. Then, the NMR shifts, δ , for $^{15}\text{N}/^{14}\text{N}$ were calculated at B3LYP/6-31+G(d,p) level resulting in the shifts shown in Table 9. Calculations have also been made on the reference nitromethane (NM), resulting in $\delta_{\text{NM}} = -120.18$, to give the experimentally significant value $\delta_{\text{NM}} - \delta$. The calculated values for *p*-dimethylaminophenylpentazole agree well with experiments. Calculations at a higher level of theory (B3LYP/6-31++G(3df,2pd)//B3LYP/6-31++G(3df,2pd)) has been performed resulting in a shift $\text{N}(\delta_{\text{NM}} - \delta) = -2.8$ for the pentazolate ion. Therefore the calculated shift for pentazolate can be expected to be accurate enough for use for experimental detection of pentazolate with ^{15}N -NMR/ ^{14}N -NMR.

Table 9 Calculated ^{15}N -NMR/ ^{14}N -NMR shifts for *p*-dimethylaminophenylpentazole and pentazolate relative to nitromethane (NM). Experimental values for pentazole[11, 40] and azide are in parenthesis[41].

		δ	$\delta_{\text{NM}} - \delta$
	N ₁	-41.66	-78.5 (-80.0)
	N ₂	-86.75	-33.4 (-27.1)
	N ₃	-129.92	9.7 (4.9)
	N ₄	197.96	-318.1 (-324.6)
	N _α	-	(-292.7)
	N _β	-	(-134.4)
	N _γ	-	(-147.0)
	N ₁	-116.56	-3.6

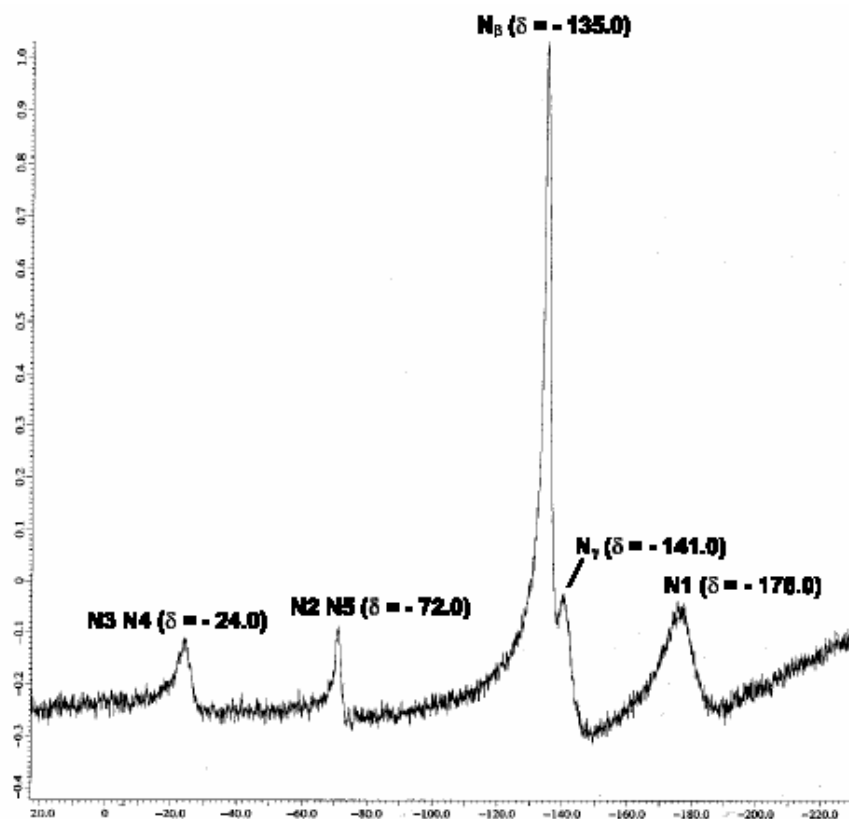


Figure 23 ^{14}N -NMR spectrum of 2,4-dichlorophenylpentazole 2,4-dichlorophenylazide and (From Reference [41])

5.4 UV spectroscopy

In order to see if any complexation or reaction is caused by the presence of metal ions in a solution of arylpentazoles it is possible to use UV spectroscopy. The UV spectra of arylpentazoles differ distinctly from the spectra of corresponding arylazides. If the pentazoles form complexes with metals, this should also be possible to see as a change in their UV spectrum. It is also possible to follow the decomposition of arylpentazoles with UV spectroscopy and the stabilisation or destabilisation of the pentazoles with presence of metal ions can be studied with kinetics measurements. We have investigated UV spectroscopy of arylpentazoles both experimentally and theoretically and this is work in progress. Complexation with metal ions and UV spectroscopy will be addressed in a future report.

5.5 Mass spectrometry

Mass spectrometry has been used to detect the pentazole anion resulting from breaking off the pentazole ring from the most stable pentazole found so far, *p*-dimethylaminophenylpentazole. This work has been performed in several steps.

First, mass spectrometry in positive mode was made and m/z 120 was detected, indicating the possibility that N_5^- may have been lost from the molecule. Later, a mass spectrometer with electrospray ionization and the capability to measure both positive and negative mass spectra was used to verify the formation of m/z -70, indicating the actual formation of N_5^- .

A disadvantage with this type of mass spectrometer and way of ionization is the need to dissolve the starting material in a solvent since it is less stable in solution than as a solid. Therefore Laser Desorption Ionization experiments with a Time-of-Flight mass spectrometer were made, first with a CO₂-laser in positive mode and later with a dye laser in negative mode.

5.5.1 Electrospray ionization

A Bruker Esquire 3000 Plus ion trap mass spectrometer was used with both positive and negative ionisation. Electrospray at a voltage of 5 kV was chosen as ionisation method since it is a gentle way to ionise thermally sensitive molecules. Nitrogen was used as collision gas and the collision energy was varied between 20 and 50 eV. Both m/z -70 corresponding to N_5^- and m/z 120 corresponding to the rest of the molecule were found (Figure 24) with negative and positive ionisation respectively. In order to use the electrospray input, the *p*-dimethylaminophenylpentazole had to be dissolved in methanol. Since the decomposition rate of all pentazoles has been found to be accelerated in solution it is preferable to use a mass spectrometer with a solid sample inlet. Initial experiments made with a Comstock Time-of-Flight (TOF) mass spectrometer using CO₂-laser evaporation of a solid sample and Electron Impact (EI) ionisation gave results similar to the positive ionisation electrospray spectra. This work has been described in a paper presented at the ICT meeting in June[4]. The results were verified in a paper by Christe and co-workers a month later[5].

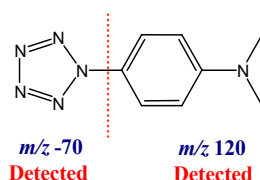


Figure 24 N_5^- has been detected in gas phase in a mass spectrometer.

5.5.2 Laser Desorption, Electron Impact Ionization with a CO₂ laser

The mass spectrometer work was continued in a more thorough study, with the TOF mass spectrometer. Among the advantages of using the TOF spectrometer is its capability to accept solid samples and use variable sorts of ionisation such as EI, laser ionisation or Laser Desorption/Ionization. A laser can be used to vaporise or vaporise and ionize the sample.

Ferrocene, which is the carbon analogue of Iron(II)pentazolate ($Fe(N_5)_2$), was studied in the TOF mass spectrometer with positive detection (Figure 25). It turned out that the vapour pressure was so high that there was no laser needed to vaporize the sample. Both m/z 121, corresponding to the ferrocene molecule without one *cyclo*-pentadiene ion, and m/z 56, corresponding to Fe^+ , was found. Also a very strong peak at m/z 186, which corresponds to the ferrocene molecule, was found even when the ionization energy was as high as -120 eV. This confirms that the molecule is very stable.

Experiments were then made with *p*-dimethylaminophenylpentazole, which was ¹⁵N labelled in the ring. The sample was dissolved in a 1:1 mixture of dichloromethane and methanol while deposited on the sample holder, followed by vacuum evaporation of the solvent before introducing the holder into the ionization chamber. A CO₂-laser was used to vaporize the sample by heating it up. Heat causes the pentazoles to decompose into the corresponding azides. The best result was obtained for the ionization energy -70 eV with 2.70 A filament current (Figure 26). The azide can be found at m/z 162 and 163. A peak at m/z 120 is expected since it corresponds to that the molecule has lost the entire pentazole ring. This peak is quite small. There is however a very strong peak at m/z 119 which is most likely due to the loss of one of the hydrogen atoms closest to the pentazole ring. The peak corresponding to the azide is quite strong, but it is impossible to say how much is caused by the laser vaporization and how much come from the EI ionization without negative detection. To see the molecular peak at m/z 191 (Figure 27) the ionization energy had to be very low, about -20 eV. This confirms that the molecule is very sensitive.

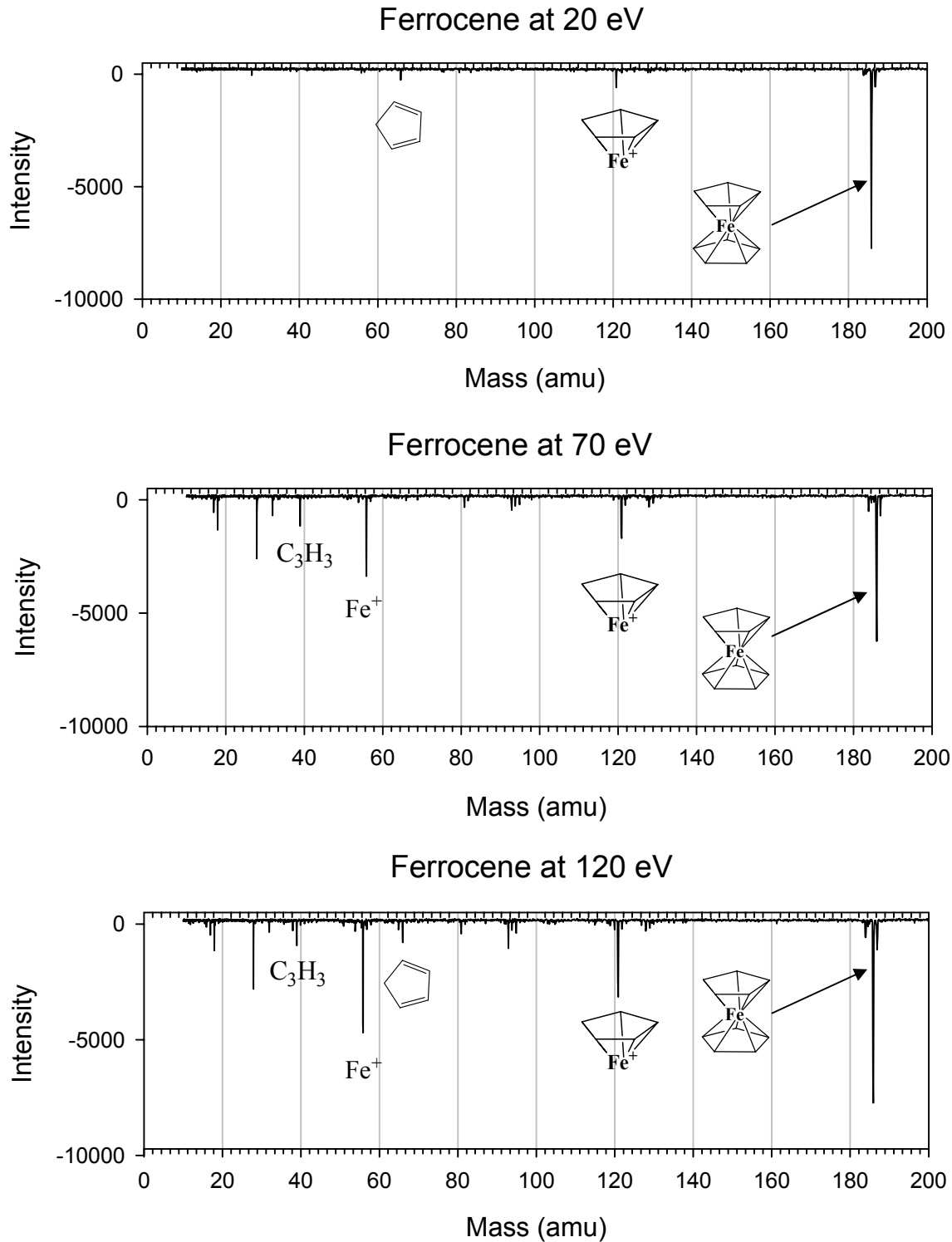


Figure 25 Mass spectra of Ferrocene at different ionization energies. The peak at 18 comes from residual water vapour in the system and the peaks at 28 and 32 come from nitrogen and oxygen respectively, due to a very small leak in the system. Only the most prominent features have been identified. Each spectrum is an average of about 860 scans and the filament current used was about 2.8 A. The pressure in the chamber was about $9 \cdot 10^{-7}$ mbar during measurement.

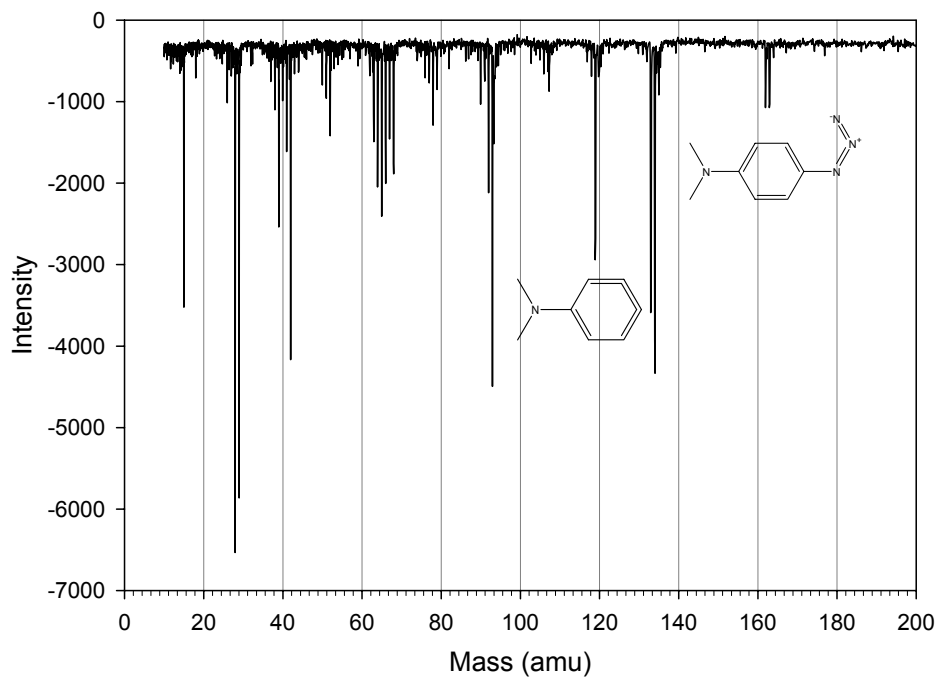


Figure 26 Mass spectrum of ^{15}N -labelled *p*-dimethylaminophenylpentazole. The peak at m/z 18 indicates presence of water. The two nitrogen peaks (N_2 and ^{15}NN) at m/z 28 and 29 respectively are not due to a leak since a corresponding peak from oxygen at m/z 32 is missing. Instead they come from the decomposition of the pentazole into azide.

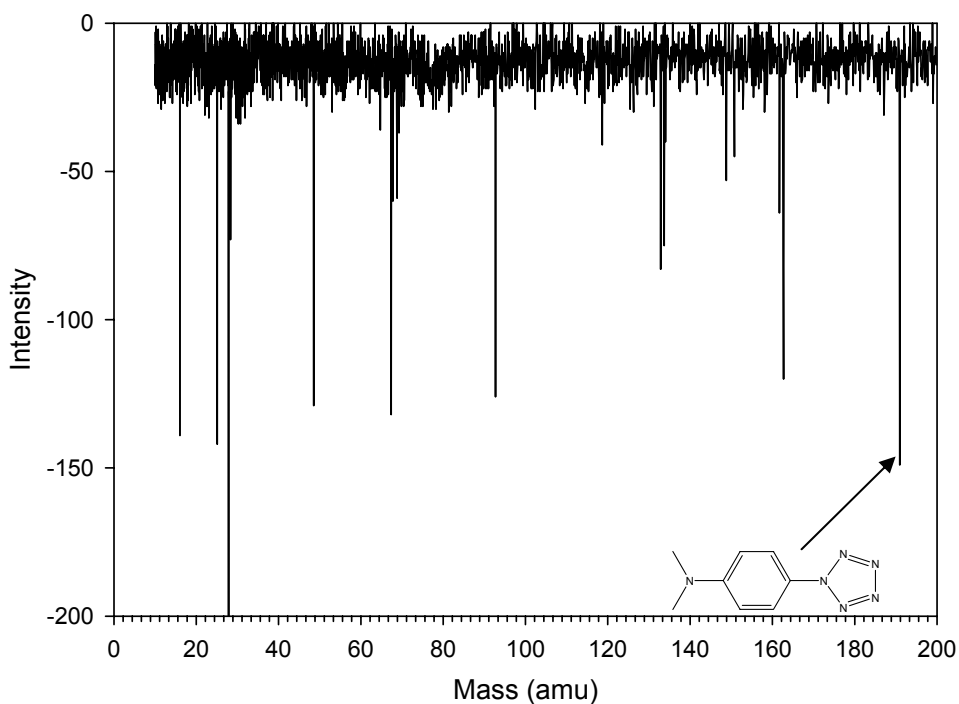


Figure 27 Mass spectrum of *p*-dimethylaminophenylpentazole. This is an average of only 100 scans where the molecular peak at m/z 191 is strong.

Observe the fact that the *p*-dimethylaminophenylazide was found at m/z 162 and 163 in equal abundance. This is proof that all azide has been formed from the decomposition of *p*-dimethylaminophenylpentazole. In this case this is not a big question, but it may provide proof of the formation of more unstable pentazoles during an attempted synthesis even though these pentazoles may not be possible to isolate. If such proof can be obtained it may be cause for an effort to break off the pentazole ring before it decomposes to azide.

5.5.3 Laser Ionization

Using a laser with short wavelength desorbs and ionizes the sample rather than just vaporising it with heat. Modification of the experimental setup to use a dye-laser in UV as well as detection of negative ions made the detection of N_5^- possible. The detection of N_5^- by Laser Desorption Ionization Mass Spectrometry has been published[3]. A more extensive description of the results is given in this chapter.

5.5.3.1 Experimental setup

An outline of the experimental setup is shown in Figure 28. The mass spectrometer setup consists of a Time-of-Flight Mass Spectrometer (TOF-MS) with custom made sample inlet and laser ionization system. The TOF-MS is a Comstock, RTOF-210/EII, equipped with CP-625C/50F Microchannel plates for ion detection. It has a mass resolution of ~ 300 in linear mode. The background pressure was $\sim 2 \cdot 10^{-6}$ mbar in the extraction chamber and $\sim 1 \cdot 10^{-7}$ mbar in the flight tube during experiments. A pulse generator, DG535, from Stanford Research Systems was used for synchronization of the laser and extraction pulses. A LeCroy LC684DL oscilloscope was used to record signals from the MCP plates.

The starting material was introduced into the vacuum chamber via a homebuilt sample inlet for pulsed laser ionization. The inlet consists of a stainless steel rod with quadratic cross section mounted on a magnetic linear and rotary motion drive. A gate valve is mounted between a small chamber, where the sample can be changed, and the main vacuum chamber. The small chamber can be pumped to about 10^{-3} mbar, which is low enough to allow opening of the gate valve into the main vacuum chamber. The *p*-dimethylaminophenylpentazole is dissolved in MeOH and kept cold in liquid N_2 , and is warmed up to above the melting point of

the solvent immediately prior to being dripped onto the holder. The solvent is evaporated off under vacuum before opening the gate valve. When inserted into the vacuum chamber, the surface of the sample holder is placed perpendicular to the laser beam.

A Lambda Physik dye laser LPD3000, pumped with a Lambda Physik Excimer laser LPX300 is used for ionization. The filament for electron ionization was turned off. The Excimer laser was set to a pulse energy of 300 mJ. The dye laser was operated at 337 nm using LC3400 dye. The measured pulse energy before attenuation was ~ 0.1 mJ. Gray filters (OD 0.1 to 2) were used to reduce the pulse energies in order to obtain good quality spectra and to vary the amount of decomposition. The laser beam is directed through the extraction chamber and focused onto the sample by a lens placed outside the vacuum chamber. The spot size is less than one millimetre in diameter.

The laser desorption ionization method offers a number of advantages in that it is in principle possible to control the amount of desorption and fragmentation by varying spot size, laser energy and laser wavelength. The draw-back is that the ionization mechanism is not fully understood [42].

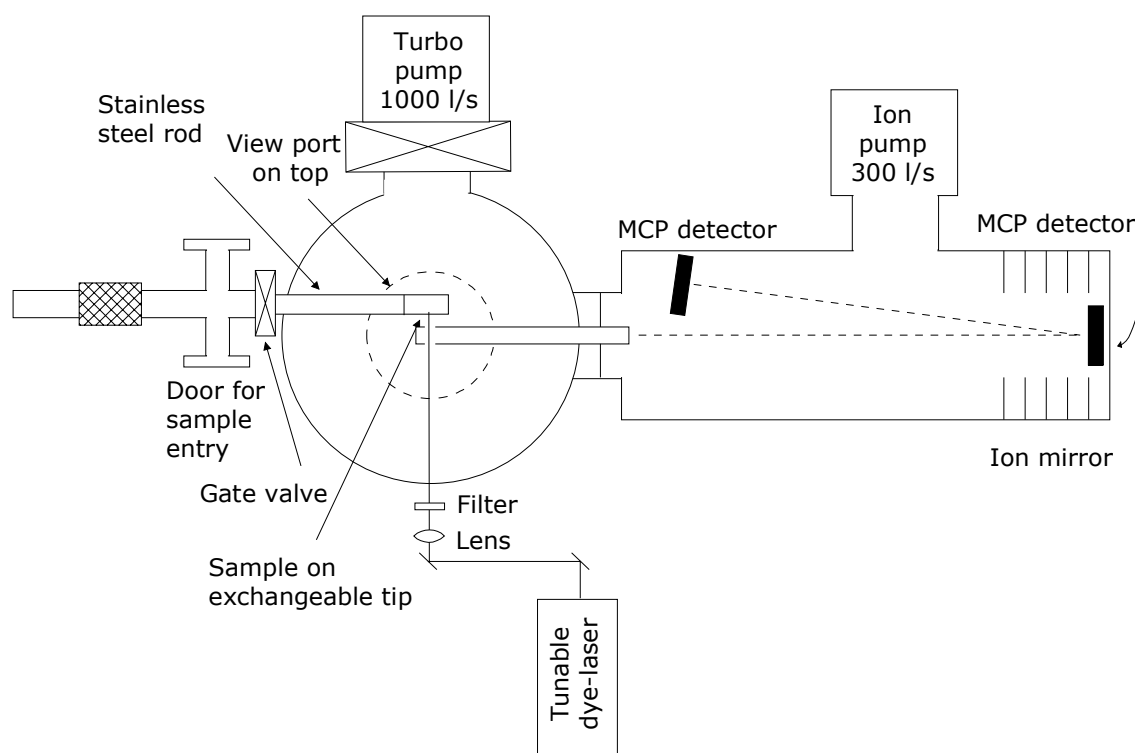


Figure 28 Schematic drawing of the mass spectrometer set-up.

5.5.3.2 Calibration

The mass spectrometer has an option to change polarity from the normal positive detection mode to negative detection mode. Calibration needs to be performed in both modes on a daily basis.

Calibration in positive mode was performed using electron impact ionization on perfluorotributylamine, also called FC-43 (Figure 29). FC-43 has prominent peaks at m/z 68.9952 (corresponding to $[\text{CF}_3]^+$), m/z 99.9936 ($[\text{C}_2\text{F}_4]^+$), m/z 130.9920 ($[\text{C}_3\text{F}_5]^+$) and m/z 218.9856 ($[\text{C}_4\text{F}_9]^+$). In addition to these peaks, m/z 28.0062 (N_2^+) is used when present.

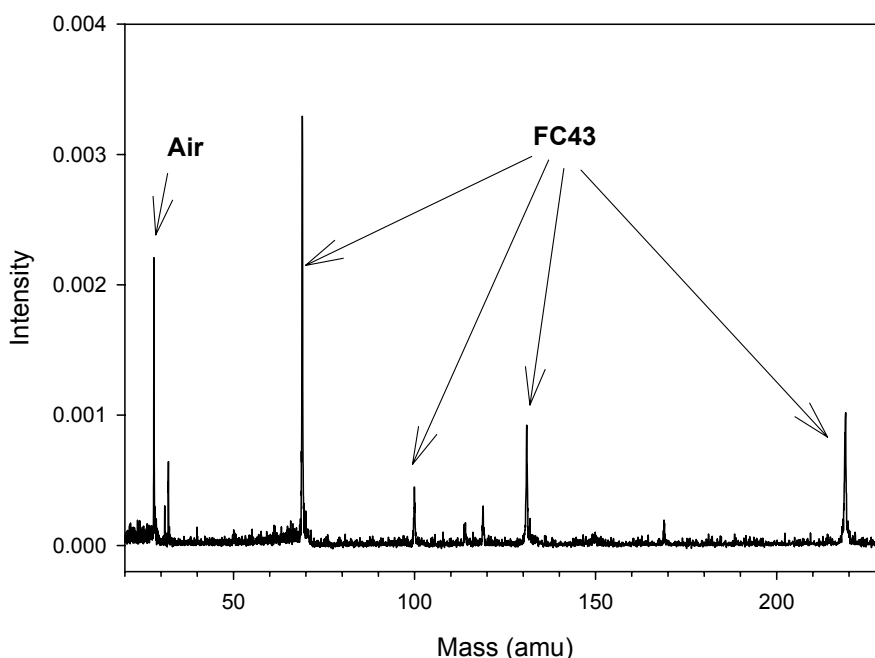


Figure 29 Mass spectrum (EI) of perfluorotributylamine (FC-43) which is used for calibration in positive mode.

Making negative ions using EI on substances like FC43 is possible but difficult. We have therefore tried a few substances that can be ionized by LDI to make our own calibration mixture. After a few attempts we decided to use a mixed sample of urea and 2,5-dihydroxybenzoic acid, DHB (Figure 30). Urea has prominent peaks at m/z -26.0031 (corresponding to CN^-), m/z -41.9980 (OCN^-) and m/z -59.0245 ($[\text{M-H}]^-$) [43] and DHB has prominent peaks at m/z -108.0210 ($[\text{M-CO}_2\text{H-H}]^-$), m/z -109.0288 ($[\text{M-CO}_2\text{H}]^-$), m/z -152.0108 ($[\text{M-2H}]^-$) and m/z -153.0186 ($[\text{M-H}]^-$) [42].

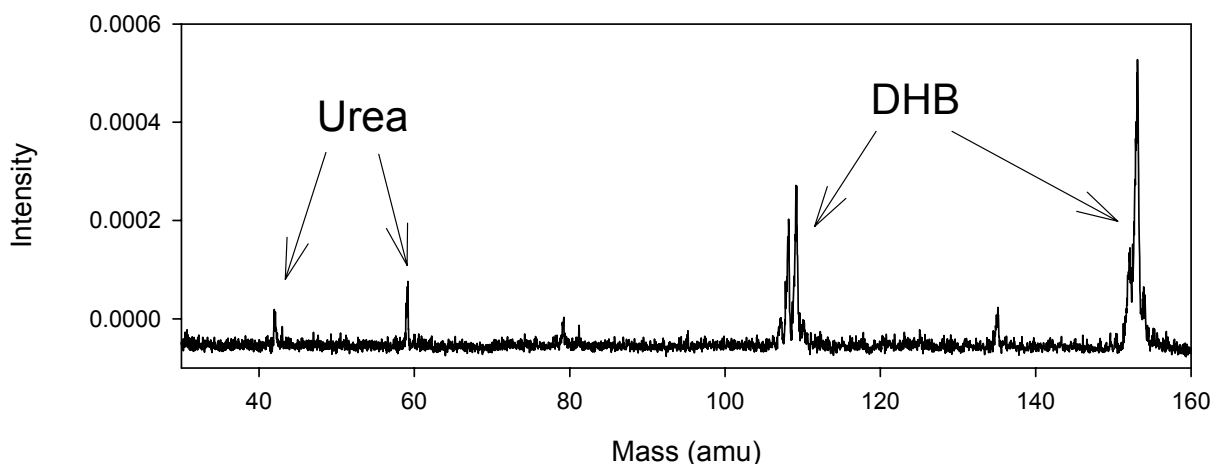


Figure 30 Mass spectrum (LDI) of a mixture of urea and 2,5-dihydroxybenzoic acid (DHB) which is used for calibration in negative mode.

5.5.3.3 Results

The *p*-dimethylaminophenylpentazole was studied using Laser Desorption Ionization (LDI) in both positive and negative detection modes in the hope of detecting *cyclo*-N₅⁻ in the negative mode. Initial experiments were performed using the positive mode and LDI (Figure 31). As expected, a fragment with *m/z* 120, corresponding to the dimethylaminobenzene cation (the loss of *cyclo*-N₅⁻ from *p*-dimethylaminophenylpentazole), was found. There was no trace of *p*-dimethylaminophenylazide cations at *m/z* 162. These two facts are strong indications that the bond between the rings in *p*-dimethylaminophenylpentazole is broken with the nitrogen ring intact, i.e. without forming the azide first. In the previously reported experiment [44] using a CO₂-laser with detection of positive fragments, there was no peak at *m/z* 120 but peaks at *m/z* 119 and *m/z* 162 and 163 (two peaks since ¹⁵N-labeled material was used). A possible explanation for the difference is that in the latter case, *p*-dimethylaminophenylpentazole decomposes into *p*-dimethylaminophenylazide as expected during heating with a CO₂-laser and that the subsequent breaking of the carbon-nitrogen bond in question involves “stealing” of one of the adjacent hydrogen atoms from the phenyl group.

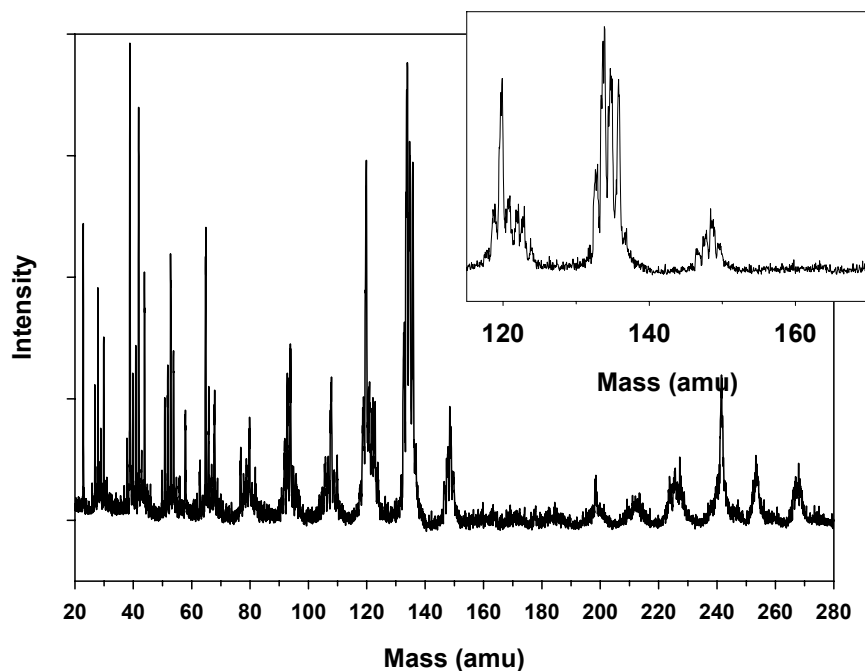


Figure 31 Mass spectrum (LDI) of *p*-dimethylaminophenylpentazole in positive mode. Notice the total absence of *p*-dimethylaminophenylazide cations. Notice also that the dimethylaminobenzene cation at m/z 120 is found in this experiment.

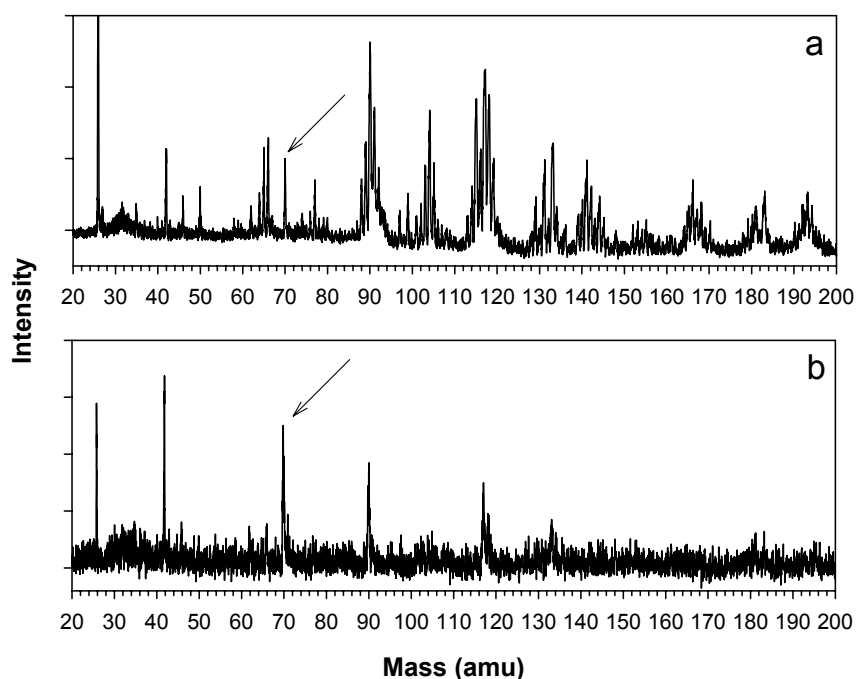


Figure 32 Negative laser ionization mass spectrum of unlabeled *p*-dimethylaminophenylpentazole at a) high energy ($\approx 80 \mu\text{J}$) b) low energy ($\approx 20 \mu\text{J}$). The arrows point out the pentazolite m/z -70 fragments.

The negative mode mass spectrum was then investigated. It was found that the fragmentation could be significantly reduced by reducing the laser power (Figure 32 a and b), giving spectra where the peaks at m/z -70 (N_5^-) and m/z -42 (N_3^-) are the strongest (Figure 32 b), apart from CN^- . The other major peaks are m/z -134, m/z -118, m/z -90 and m/z -26 ($[CN]^-$).

To verify that the ion at m/z -70 was in fact the pentazolate anion, measurements on isotopic labelled *p*-dimethylaminophenylpentazole were made using monolabelled material with ^{15}N in the 2 position and dilabelled material with ^{15}N in either the 2 and 3 or 2 and 5 positions in the pentazole ring. The negative mass spectrum using the monolabelled *p*-dimethylaminophenylpentazole gives a peak at m/z -71 (Figure 33) corresponding to the ^{15}N -labelled pentazolate anion as expected. Further evidence that the pentazolate anion is present can be obtained from the intensity of the azide signals at m/z -42 and m/z -43 corresponding to the $^{14}N_3$ and $^{15}N^{14}N_2$ ions respectively. If the azide ion was a result of fragmentation of the pentazole directly, then the two signals would be of equal intensity. However, if the azide ion was the result of the pentazolate anion undergoing fragmentation, then the intensity of the ratio of signal intensities at m/z -42 and m/z -43 would be 2:3. This is clearly seen in Figure 33. In further investigations using the dilabelled material the ^{15}N dilabelled pentazolate anion peak was observed at m/z -72 and peaks corresponding to the azide ion were observed at m/z -42, m/z -43 and m/z -44 as expected (Figure 33). We conclude that the m/z -70 is the *cyclic*- N_5^- since the open-chain N_5^- is not stable [45].

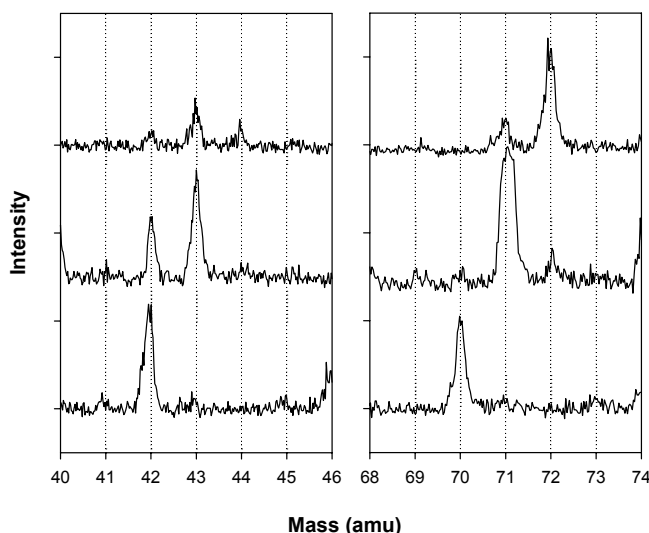


Figure 33 A close-up of the azide ion and pentazolate anion regions of the negative laser ionization mass spectrum of ^{15}N dilabelled (upper trace), ^{15}N monolabelled (middle trace) and unlabeled (lower trace) *p*-dimethylaminophenylpentazole.

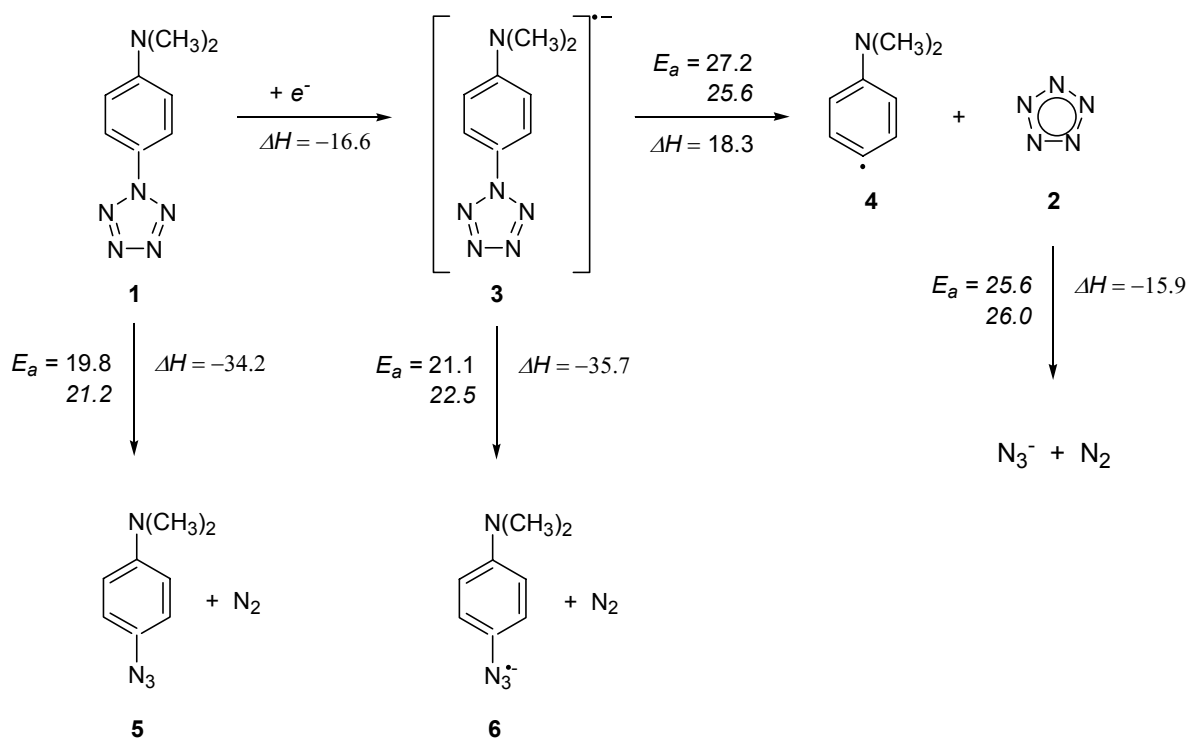
5.5.3.4 QM calculations

The details of the mechanisms for producing ions and fragments by UV-laser radiation are not fully understood [42, 43], but our results clearly demonstrate the selectivity and efficiency of the LDI-TOF-MS method. It is shown that the combination of a solid sample inlet with pulsed UV-laser decomposition and ionization leads to a selective cleavage of the bond connecting the two ring systems and production of **2** when using optimized laser energy (Scheme 8).

On increasing the laser power, the degree of fragmentation increases and other decomposition products due to cleavage of the aromatic ring are observed (Figure 32a). In the negative mass spectra we observe peaks from the pentazolate and dimethylaminophenyl structures respectively but even at higher laser power no mixed anionic fragments due to cleavage of the nitrogen ring are formed, as determined from the ^{15}N labeling experiments. Furthermore, the molecular $[\text{M}]^-$ and $[\text{M}-\text{N}_2]^-$ anions could not be observed, indicating that the reaction mechanism is highly selective towards cleavage of **2** from **1** and the decomposition is very fast. The N_3^- observed in the experiment is almost exclusively formed by decomposition of **2**. The relatively high $\text{N}5^-:\text{N}3^-$ ratio also indicates a high stability of **2**. An interesting feature of the negative mass spectra is the strong CN^- peak, which is observed even at the lower laser intensity (Figure 32b). The CN^- formation is likely due to the ionization process where some molecules are highly fragmented, producing a plasma containing ions, which helps further ionization and fragmentation of other molecules.

On the basis of the observed spectral features and quantum chemical calculations, we conclude that the most likely mechanism for forming **2** is an electron attachment to **1** followed by a carbon-nitrogen bond cleavage of the radical anion (**3**) to form *p*-dimethylaminophenyl radical (**4**) and **2**. The homolytic cleavage of **1** to form **4** and $\text{N}5^\bullet$, followed by an electron attachment to $\text{N}5^\bullet$ is a much less likely process due to a much higher energy barrier. In addition $\text{N}5^\bullet$ is very unstable [45] and not likely to live long enough to capture an electron.

To summarize, we have demonstrated that the presented method based on a solid sample inlet combined with pulsed UV-laser decomposition and ionization can be used for selective production of pentazolate anions. This method has far better potential than the LC/MS method used in previous work [4, 5], and it opens up the possibility for characterization of **2** by other methods, such as matrix isolation spectroscopy (MIS).



Scheme 8 Decomposition pathway of *p*-dimethylphenylpentazole. Activation energies (E_a) and enthalpies (ΔH) are at 298 K and in kcal/mol. Values are computed at the B3LYP/6 311+G(2df,p) and G2X (in italics) levels. Molecular weights are given in parenthesis.

5.5.3.5 Discussion and conclusions

The details of the mechanisms for producing ions and fragments by UV-laser radiation are not fully understood [42, 43], but our results clearly demonstrate the selectivity and efficiency of the LDI-TOF-MS method. It is shown that the combination of a solid sample inlet with pulsed UV-laser decomposition and ionization leads to a selective cleavage of the bond connecting the two ring systems and production of **2** when using optimized laser energy.

On increasing the laser power, the degree of fragmentation increases and other decomposition products due to cleavage of the aromatic ring are observed (Figure 32a). In the negative mass spectra we observe peaks from the pentazolate and dimethylaminophenyl structures respectively but even at higher laser power no mixed anionic fragments due to cleavage of the nitrogen ring are formed, as determined from the ^{15}N labeling experiments. Furthermore, the molecular $[\text{M}]^-$ and $[\text{M}-\text{N}_2]^-$ anions could not be observed, indicating that the reaction mechanism is highly selective towards cleavage of **2** from **1** and the decomposition

is very fast. The N_3^- observed in the experiment is almost exclusively formed by decomposition of **2**. The relatively high $N_5^-:N_3^-$ ratio also indicates a high stability of **2**. An interesting feature of the negative mass spectra is the strong CN^- peak, which is observed even at the lower laser intensity (Figure 32b). The CN^- formation is likely due to the ionization process where some molecules are highly fragmented, producing a plasma containing ions, which helps further ionization and fragmentation of other molecules.

On the basis of the observed spectral features and quantum chemical calculations, we conclude that the most likely mechanism for forming **2** is an electron attachment to **1** followed by a carbon-nitrogen bond cleavage of the radical anion (**3**) to form *p*-dimethylaminophenyl radical (**4**) and **2**. The homolytic cleavage of **1** to form **4** and N_5^\bullet , followed by an electron attachment to N_5^\bullet is a much less likely process due to a much higher energy barrier. In addition N_5^\bullet is very unstable [45] and not likely to live long enough to capture an electron.

To summarize, we have demonstrated that the presented method based on a solid sample inlet combined with pulsed UV-laser decomposition and ionization can be used for selective production of pentazolate anions. This method has far better potential than the LC/MS method used in previous work [4, 5], and it opens up the possibility for characterization of **2** by other methods, such as matrix isolation spectroscopy (MIS).

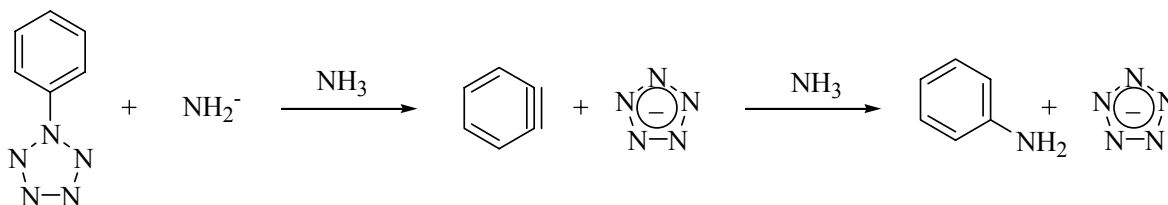
5.5.3.6 Future experiments

The experiments made so far have shown that it is indeed possible to selectively break the C-N bond between the two rings, but also that it is highly dependent on the experimental conditions such as laser power.

A natural next step is to put pentazolate into a matrix in order to be able to do spectroscopic studies. However, doing so there are no means of knowing how much pentazolate anions we produce until there is a sufficient amount on the window for spectrometric measurement. This means that the exact conditions, under which as much *cyclo-N₅⁻* as possible is formed needs to be investigated and mastered. This is best done continuing with the mass spectrometry setup, systematically investigating the influence of for example laser power and laser wavelength on the resulting mass spectrum. Our measurements so far indicate that there is only a very narrow region between too low laser power (i.e. nothing happens) and too high laser power (i.e. leading to high fragmentation).

6 Benzyne reaction or amination of arylpentazoles

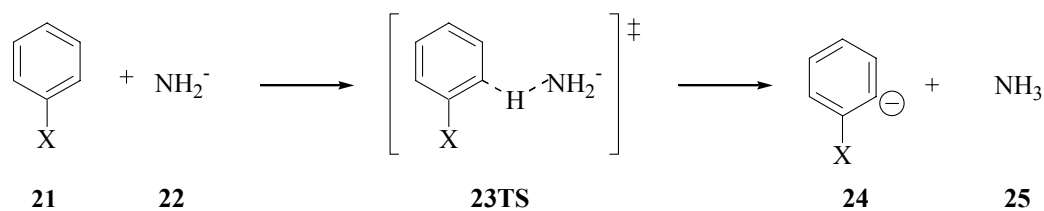
A “wet chemistry” route using arylpentazoles as starting material for the isolation of the pentazolate anion is a nucleophilic aromatic substitution. The reaction in Scheme 9 is well understood when the substituent is a halogen such as bromide or chloride and proceeds through the interesting and much studied intermediate benzyne. The reaction is performed with excess of sodium or potassium amide in liquid ammonia at -33°C . The low temperature gives the extra advantage of a more stable product. The benzyne mechanism is characterized by removal of the proton ortho to the halogen by the basic amide (halobenzenes with no ortho-hydrogens fail to react). In the next step of the reaction the halogen leaves the intermediate anion (*o*-halophenyl anion) producing the highly reactive benzyne intermediate. Finally the benzyne reacts with ammonia to form the product aniline. To investigate if this reaction could be a plausible alternative for the isolation of the pentazolate anion, we have studied the first two steps of the amination reaction for chlorobenzene, bromobenzene, and fluorobenzene leading to the formation of the benzyne intermediate. Of the three halobenzenes, fluorobenzene is known not to proceed to products[46]. The results are compared to those for the phenylpentazole to evaluate if this is a possible route to isolate the pentazolate anion, *cyclo-N₅⁻*.



Scheme 9 Nucleophilic Aromatic Substitution reaction in liquid ammonia at -33°C .

6.1 The proton transfer step

The results for the first step, the proton transfer step (Scheme 10) are presented in Table 10 and Table 11. Results from the formation of the benzyne intermediate (Scheme 11) are presented in Table 12.



Scheme 10 The proton transfer step in the benzyne-reaction

Table 10 Relative energies (kcal/mol) for the transition state for the proton transfer^a

	ΔE^\ddagger (B3LYP)	ΔE^\ddagger (MP2)	ΔH_g°	ΔG_g°	$\Delta G_{\text{sol}}^\circ$
Br	-16.6	-16.0	-18.4	-11.7	15.7
Cl	-15.2	-14.8	-17.2	-10.8	16.6
F	-14.3	-14.8	-16.4	-10.1	16.6
<i>cyclo-N₅</i>	-22.5	-25.0	-24.5	-17.5	16.4

^aThe definitions for the energetics (with respect to the reactants 3 are: ΔE : classical energy, $\Delta H_g^\circ = \Delta E(\text{B3LYP}) + \Delta \Delta H_g$, where $\Delta \Delta H_g$ is the enthalpy correction. $\Delta G_g^\circ = \Delta E(\text{B3LYP}) + \Delta \Delta G_g$, where $\Delta \Delta G_g$ is the free energy correction. $\Delta \Delta G_g$ and $\Delta \Delta H_g$ is calculated at 240.15 K and 1 atm, with the vibrational frequencies obtained at the B3LYP/6-31+G* level. $\Delta G_{\text{sol}}^\circ = \Delta G_g^\circ + \Delta \Delta G(1 \text{ atm} \rightarrow 1 \text{ M}) + \Delta \Delta G_{\text{sol}}$. $\Delta \Delta G_{\text{sol}}$: PCM solvation free energy correction. $\Delta \Delta G(1 \text{ atm} \rightarrow 1 \text{ M})$ is the correction factor (1.42 kcal/mol per molecule) for changing the standard state from 1 atm to 1 M. The $\Delta G_{\text{sol}}^\circ$ values correspond to a standard state of 1 M solution in a solvent which has the same properties as pure ammonia.

Table 11 Relative energies (kcal/mol) for the products of the proton transfer^a

	$\Delta E(\text{B3LYP})$	$\Delta E(\text{MP2})$	ΔH_g°	ΔG_g°	$\Delta G_{\text{sol}}^\circ$
Br	-20.1	-19.9	-19,3	-20.3	7.8
Cl	-18.7	-17.8	-18,0	-18.9	7.7
F	-17.0	-19.4	-16,3	-17.1	7.0
N ₅	-29.0	-33.0	-28,2	-29.2	4.6

^aFor definitions see Table 10.

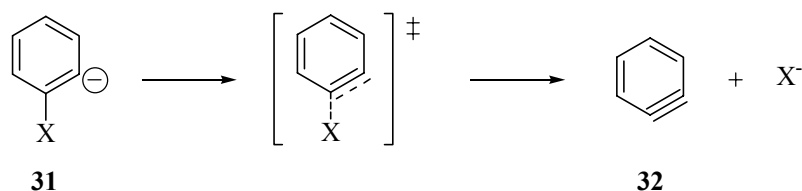
The computed B3LYP free energies of activation for the proton transfer are close to 16 kcal/mol for all the studied species. This is in relatively good agreement with the experimental free energy of activation for fluorobenzene, which can be estimated to 14.4 kcal/mol from the rate constant of proton exchange for amide anions in liquid ammonia[47]. The discrepancy of 2.2 kcal/mol between theory and experiment is within the

expected error of the B3LYP method. The result is even more encouraging considering that we are likely overestimate the entropy cost of bringing the reactants together by a few kcal/mol by using the gas phase expression in the calculation of the translational and rotational entropies. The overall proton transfer reaction is endergonic by 7-8 kcal/mol for the halobenzenes after consideration of solvent effects, which is consistent with the fact that the *o*-halobenzene anion has not been detected as a stable intermediate.

Comparing the energetics for the phenylpentazole with those of the halobenzenes shows that phenylpentazole is considerably more reactive in gas phase. This can be attributed to the large electron-withdrawing capacity of the pentazole substituent. The difference in energetics compared to the halobenzenes is essentially absent after consideration of solvation effects. The activation energy in solution of 16.6 kcal/mol is almost identical to that of the chlorobenzene and fluorobenzene. However, the overall reaction is less endergonic for the phenylpentazole than for the halobenzenes by around 3 kcal/mol. Interestingly, in contrast to the results for the halobenzenes we find significant differences between B3LYP and MP2 relative energies. The latter method lowers the activation energy by 2.5 kcal/mol and the reaction energy by 4.0 kcal/mol. Taken together the B3LYP and MP2 results strongly indicates that the proton transfer should be equally or even more favourable for the phenylpentazole as for the halobenzenes. It is even possible that the ortho-phenylpentazole anion is sufficiently stable (see 4.2.4) to facilitate its detection.

6.2 Benzyne formation

The second part of the benzyne reaction, the formation of the benzyne intermediate (Scheme 11) is highly dependent on solvent effects. The halogen/pentazole leaves the benzene ring concerted with the formation of a triple bond. This step is driven by the solvation of the leaving negative ion, and it is not possible to find a gas phase transition state. Instead we have estimated the solution transition state directly using a step-wise constrained solvent optimization (Table 12). The free energy of activation increases in the order Br < Cl << F with the values 2.9, 5.4 and 29.0 kcal/mol, respectively. The very high activation energy for fluorobenzene is consistent with the observation that this reaction does not proceed to products.



Scheme 11 The second step in the benzyne reaction, formation of benzyne.

Table 12 Relative B3LYP/6-31+G* energies for the second step of the benzyne reaction, estimated from a constrained stepwise optimization, all energies in kcal/mol^a.

	$\Delta G_{\text{sol}}^{\ddagger}$
Br	2.7
Cl	5.4
F	29.0
N ₅	25.3

^a Activation energies estimated from the scan function in Jaguar 4.1, 20 points were scanned using a step size of 0.1 Å, all points in the scan are fully optimized (B3LYP/6-31+G* and LACVP*+ for bromobenzene) with solvation effects added.

The estimated free energy of activation for the benzyne formation of phenylpentazole is 25.3 kcal/mol, which is a little too high to make the reaction useful for synthesis, considering that the proton transfer step is slightly endergonic (4.7 kcal/mol and 0.7 kcal/mol at the B3LYP and MP2 levels, respectively). However, it should be noted that we do not account for the vibrational effects on the activation energy for this step. These usually lower the activation energy by a few kcal/mol, due to the conversion of one of the vibrational degrees of freedom to a translation upon passing the transition state. There is also some uncertainty in the computed energies and it is not unlikely that we in total may overestimate the overall activation energy by 4-5 kcal/mol. This could make the reaction feasible. The activation energy for this step could also be influenced by a substituent on the phenyl group, preferably an electron donating substituent, such as NH₂, which would be expected to lower the energy of the transition state relative the intermediate. However, after scanning the potential energy for the *p*-NH₂ substituted phenylpentazole, a similar activation energy was obtained. We are also limited to the use of electron donating substituents para to the pentazole ring in order to achieve a stable reactant.

6.3 Lowering the activation energy with metal complex

The most promising route to use the benzyne mechanism for the isolation of the all-nitrogen anion is to add a complexing metal cation. The very polar phenylpentazole has most of its negative charge centred on the pentazole, making this an attractive target for complexing metals such as Fe^{2+} and Zn^{2+} as suggested in a recent article [6]. The metal binds in the plane of the ring and coordinates to the 3 nitrogen. This is likely to increase the stability of phenylpentazole anion to leave in the second step, lowering the activation energy. It also has the added benefit of producing a complexed pentazolite anion, which would be easier to isolate and/or detect. We investigated the benzyne formation with a Zn^{2+} complexed to the 3 position of the pentazole ring (Figure 34). This resulted in a reduction of the free energy of activation for this step by more than 6 kcal/mol. The activation free energy of 19.0 kcal/mol is sufficiently low to make the reaction of interest for synthesis; in particular if it is performed in an alternative solvent that allows a higher reaction temperature. After removal of the solvent one would expect to find the complex $\text{Zn}(\text{N}_5)_2$ or mixed complexes, such as $\text{Zn}(\text{Cl})\text{N}_5$. In order to facilitate the detection of these complexes, we have calculated their spectroscopic properties and the results are presented in the next section.

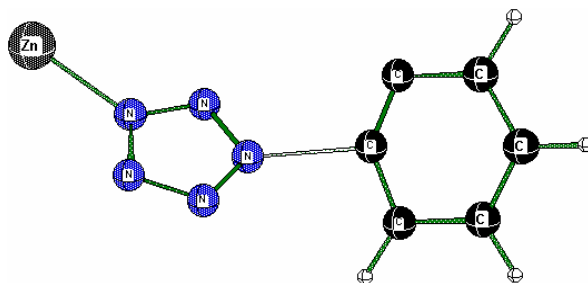


Figure 34 Zn^{2+} complexed with phenylpentazole, transition state structure.

7 Conclusions

The work on N_5^- is progressing well. The successful detection of N_5^- in a mass spectrometer, which is a breakthrough in the research of all-nitrogen chemistry, strengthens our belief that synthesis of the pentazolate anion and its salts will be a feasible task. Work continues towards the synthesis of N_5^- in form of a metal salt in solution or in solid state. Some detection methods suitable for N_5^- are available. Research at FOI has shown that all-nitrogen HEDM and especially N_4 and N_5^- are reasonable targets. The performance expected from these compounds is about 1.5 to 3 times the performance of HMX.

8 References

1. Wallin, S., et al., *High Energy Density Materials (HEDM) - A literature survey*. 2004, Swedish Defence Research Agency, FOI: Stockholm.
2. Christe, K.O., et al., N_5^+ : *A Novel Homoleptic Polynitrogen Ion as a High Energy Density Material*. *Angew. Chem. Int. Ed.*, 1999. **38**(13/14): p. 2004-2009.
3. Östmark, H., et al., *Detection of pentazolate anion (cyclo- N_5^-) from laser ionization and decomposition of solid p-dimethylaminophenylpentazole*. *Chemical Physics Letters*, 2003. **379**: p. 539-546.
4. Hahma, A., et al. *Synthesis and Characterization of Phenylpentazoles*. in *33rd International Annual Conference of ICT*. 2002. Karlsruhe.
5. Vij, A., et al., *Experimental Detection of the Pentaazacyclopentadienide (Pentazolate) Anion, cyclo- N_5^-* . *Angewandte Chemie International Edition*, 2002. **41**(16): p. 3051-3053.
6. Butler, R.N., J.C. Stephens, and L.A. Burke, *First generation of pentazole (HN_5 , pentazolic acid), the final azole, and a zinc pentazolate salt in solution: A new N-dearylation of 1-(p-methoxyphenyl) pyrazoles, a 2-(p-methoxyphenyl) tetrazole and application of the methodology to 1-(p-methoxyphenyl) pentazole*. *Chem. Commun.*, 2003: p. 1016-1017.
7. Hantzsch, A., *Ber. d. Chem. Ges.*, 1903. **36**: p. 2056.
8. Huisgen, R. and I. Ugi, *Zur Lösung eines klassischen Problems der organischen Stickstoff-Chemie*. *Angew. Chem.*, 1956. **68**: p. 705-706.
9. Nguyen, M.T., et al., *Can The Pentazole anion (N_5^-) be Isolated and/or Trapped in Metal Complexes*. *Polyhedron*, 1985. **4**(10): p. 1721-1726.
10. Glukhovtsev, M. and P.v.R. Schleyer, *The N_4 Molecule Has an Open-Chain Triplet C_{2h} Structure*. *Int. J. Quantum Chem.*, 1993. **46**: p. 119-125.
11. Burke, L.A.B., Richard N.; Stephens, John C., *Theoretical characterization of pentazole anion with metal counter ions. Calculated and experimental ^{15}N shifts of aryldiazonium, -azide and -pentazole systems*. *J. Chem. Soc., Perkin Trans. 2*, 2001: p. 1679-1684.
12. Lein, M., et al., *Iron Bispentazole $Fe(\eta^5-N_5)_2$, a Theoretically Predicted High-Energy Compound: Structure, Bonding Analysis, Metal - Ligand Bond Strength and a Comparison with the Isoelectronic Ferrocene*. *Chem. Eur. J.*, 2001. **7**(19): p. 4155-4163.
13. Straka, M. and P. Pyykkö, *One Metal and Forty Nitrogens. Ab initio Predictions for Possible New High-Energy Pentazolides*. *Inorganic Chemistry*, 2003. **42**: p. 8241-8249.
14. Tsipis, A.C. and A.T. Chaviara, *Structure, Energetics, and Bonding of First Row Transition Metal Pentazolato Complexes: A DFT Study*. *Inorg. Chem.*, 2004. **43**: p. 1273-1286.
15. Brinck, T., et al., *Energetic Materials Research for Singapore. Progress during the second year*. 2004, Swedish Defence Research Agency, FOI: Tumba. p. 570.
16. Urnežius, E., et al., *Science*, 2002. **295**: p. 834-835.
17. Lein, M., J. Frunzke, and G. Frenking, *Structures and Bonding of the Sandwich Complexes*. *Inorg. Chem.*, 2003. **42**: p. 2504-2511.
18. Glukhovtsev, M.N., P.v.R. Schleyer, and C. Maerker, *Pentaaza- and Pentaphosphacyclopentadienide Anions and Their Lithium and Sodium Derivatives: Structures and Stabilities*. *J. Phys. Chem.*, 1993. **97**: p. 8200-8206.

19. Fau, S., K.J. Wilson, and R.J. Bartlett, *On the Stability of $N_5^+N_5^-$* . Journal of Physical Chemistry, 2002. **106**: p. 4639-4644.
20. Fau, S., K.J. Wilson, and R.J. Bartlett, *Correction: On the Stability of $N_5^+N_5^-$* . Journal of Physical Chemistry, 2004. **108**(1): p. 236.
21. Evangelisti, S. and T. Leininger, *Ionic nitrogen clusters*. Journal of Molecular Structure (Theochem), 2003. **621**: p. 43-50.
22. Bemm, U. and H. Östmark, *Structure of 1,1-diamino-2,2-dinitroethylene: A novel Energetic Material with Infinite Layers in Two Dimensions*. Acta Crystallogrpy, 1998. **C54**.
23. Dixon, D.A., et al., *Enthalpies of Formation of Gas-Phase N_3, N_3^-, N_5^+ , and N_5^- from Ab Initio Molecular Orbital Theory, Stability Predictions for $N_5^+N_3^-$ and $N_5^+N_5^-$, and Experimental Evidence for the Instability of $N_5^+N_3^-$* . J. Am. Chem. Soc., 2004. **126**: p. 834-843.
24. Ugi, I. and R. Huisgen, *Pentazole II. Die Zerfallsgeschwindigkeit der Arylpentazole*. Chem. Ber., 1958. **91**: p. 531-537.
25. Huisgen, R. and I. Ugi, *Pentazole I. Die Lösung eines klassischen Problems der organischen Stickstoffchemie*. Chem. Ber., 1957. **90**: p. 2914-2927.
26. Ugi, I., et al., *Zur Reaktion des Benzol-diazonium-Ions mit Azid Nachweis des Phenylpentazols als Zwischenstufe*. Angew Chem, 1956. **68**(23): p. 753-754.
27. Ugi, I., H. Perlinger, and L. Perlinger, *Pentazole, III Kristallisierte Aryl-pentazole*. Chem. Ber., 1958. **91**: p. 2324-2329.
28. Ugi, I., *Pentazole V. Zum Mechanismus der Bildung und des Zerfalls von Phenylpentazol*. Tetrahedron, 1963: p. 1801-1803.
29. Benin, V., P. Kaszynski, and J.G. Radziszewski, *Arylpentazoles Revisited: Experimental and Theoretical Studies of 4-Hydroxyphenylpentazole and 4-Oxyphenylpentazole Anion*. Journal of Organic Chemistry, 2002. **67**: p. 1354-1358.
30. Ugi, I., H. Perlinger, and L. Behringer, *Pentazole IV. der konstitutionsbeweis für fristallisiertes [p-Äthoxy-phenyl]-pentazol*. Chemische Berichte, 1959. **92**: p. 1864-1866.
31. Müller, R., J.D. Wallis, and W.v. Philipsborn, *Direkter Strukturbeweis für das Pentazol-Ringsystem in Lösung durch ^{15}N -NMR-Spektroskopie*. Angewandte Chemie, 1985. **97**: p. 515-517.
32. Wallis, J.D. and J.D. Dunitz, *An All-nitrogen Aromatic Ring System: Structural Study of 4-Dimethylaminophenylpentazole*. J. Chem Soc., Chem Commun., 1983: p. 910-911.
33. Carlqvist, P., H. Östmark, and T. Brinck, *The Stability of Arylpentazoles*. Journal of Physical Chemistry A, 2004. **108**: p. 7463-7467.
34. Hammerl, A. and T.A. Klapötke, *Tetrazolypentazoles: Nitrogen-Rich Compounds*. Inorg. Chem., 2002. **41**(4): p. 906-912.
35. Bieseimer, F., K. Harms, and U. Müller, *Pentazol-Derivate und daraus entstehende Azide: [O3S-p-C6H4-N5]- und [O3S-p-C6H4-N3]- als Kalium-Kronenether-Salze*. Z. Anorg. Allg. Chem., 2004. **630**: p. 787-793.
36. Demtröder, W., *Laser Spectroscopy*. 3rd ed. 2002: Springer Verlag.
37. Perera, S.A. and R.J. Bartlett, *Coupled-cluster calculations of Raman intensitie and their application to N_4 and N_5^-* . Chem. Phys. Lett., 1999. **314**: p. 381-387.
38. Östmark, H., et al., *On the possibility of detecting tetraazatetrahedrane (N_4) in liquid or solid nitrogen by Fourier transform Raman spectroscopy*. J. Raman Spectr., 2001. **32**(3): p. 195-199.

39. Butler, R.N., S. Collier, and A.F.M. Fleming, *Pentazoles: proton and carbon-13 NMR spectra of some 1-arylpentazoles: kinetics and mechanism of degradation of the arylpentazole system*. J. Chem. Soc., Perkin Trans. 2, 1996: p. 801-803.
40. Butler, R.N.F., Anthony; Collier Seamus; Burke, Luke A., *Pentazole chemistry: the mechanism of the reaction of aryldiazonium chlorides with azide ion at -80 °C: concerted versus stepwise formation of arylpentazoles, detection of a pentazene intermediate, a combined ¹H and ¹⁵N NMR experimental and ab initio theoretical study*. J. Chem. Soc., Perkin Trans. 2, 1998: p. 2243-2247.
41. Adam, D., *The synthesis and characterisation of halogen and nitro phenyl azide derivatives as highly energetic materials.*, in *Fakultät für Chemie und Pharmazie*. 2001, Ludwig-Maximilians-Universität: München. p. 211.
42. Bourcier, S., S. Bouchonnet, and Y. Hoppilliard, *Ionization of 2,5-dihydroxybenzoic acid (DHB) matrix-assisted laser Desorption ionization experiments and theoretical study*. Int. J. Mass Spectrom., 2001. **210/211**: p. 59-69.
43. Pshenichnyuk, S.A., et al., *Temperature dependencies of negative ions formation by capture of low-energy electrons for some typical MALDI matrices*. Int. J. Mass Spectrom., 2003. **227:2**: p. 259-272.
44. Bergman, H., et al., *Energetic materials research for Singapore. Progress during the first year*. 2003: Stockholm.
45. Nguyen, M.T. and T.-K. Ha, *Decomposition mechanism of the polynitrogen N₅ and N₆ clusters and their ions*. Chemical Physics Letters, 2001. **335**: p. 311-320.
46. Roberts, J.D., et al., *The Mechanism of Aminations of Halobenzenes*. J. Am. Chem. Soc., 1955. **78**: p. 601-611.
47. Hall, G.E., R. Piccolini, and J.D. Roberts, *Exchange Reactions of Deuterated Benzene Derivatives with Potassium Amide in Liquid Ammonia*. JACS, 1955. **77**: p. 4540-4543.

Issuing organization FOI – Swedish Defence Research Agency Weapons and Protection SE-147 25 Tumba	Report number, ISRN FOI-R--1602--SE	Report type Technical report
	Research area code 5. Strike and protection	
	Month year March 2005	Project no. E2004
	Sub area code 51 Weapons and Protection	
	Sub area code 2	
Author/s (editor/s) Sara Wallin Arno Hahma Henric Östmark Emma Hedlund Tore Brinck Erik Holmgren Peter Carlqvist Martin Norrefeldt Rob Claridge Larisa Yudina Lars Eriksson	Project manager	
	Approved by	
	Sponsoring agency	
	Scientifically and technically responsible	
Report title High Energy Density Materials Efforts to synthesize the pentazolate anion: Part 1		
Abstract (not more than 200 words) The report describes the progress in the work to synthesise the pentazolate anion, N_5^- . The starting materials, arylpentazoles, and their properties are discussed. Detection methods including the successful detection with mass spectrometry are described. The results of quantum mechanical calculations on a possible wet chemistry route to make N_5^- are also presented.		
Keywords HEDM, N_5^- , Syntehsis		
Further bibliographic information	Language English	
ISSN 1650-1942	Pages 64 p.	
	Price acc. to pricelist	

Utgivare Totalförsvarets Forskningsinstitut - FOI Vapen och skydd 147 25 Tumba	Rapportnummer, ISRN FOI-R--1602--SE	Klassificering Teknisk rapport
	Forskningsområde 5. Bekämpning och skydd	
	Månad, år Mars 2005	Projektnummer E2004
	Delområde 51 VVS med styrda vapen	
	Delområde 2	
Författare/redaktör Sara Wallin Arno Hahma Henric Östmark Emma Hedlund Tore Brinck Erik Holmgren Peter Carlqvist Martin Norrefeldt Rob Claridge Larisa Yudina Lars Eriksson	Projektledare	
	Godkänd av	
	Uppdragsgivare/kundbeteckning	
	Tekniskt och/eller vetenskapligt ansvarig	
Rapportens titel (i översättning) HEDM, Försök att syntetisera pentazolanjonen: Del 1		
Sammanfattning (högst 200 ord) Rapporten beskriver framstegen i arbetet med att syntetisera pentazolanjonen, N ₅ ⁻ . Startmaterialen, arylpentazoler, och deras egenskaper beskrivs. Detektionsmetoder, inklusive den lyckade detektionen i en masspektrometer diskuteras också. Resultat från kvantmekaniska beräkningar på en möjlig våtkemisk syntesväg till N ₅ ⁻ presenteras också.		
Nyckelord HDEM, N5-, Syntes		
Övriga bibliografiska uppgifter	Språk Engelska	
ISSN 1650-1942	Antal sidor: 64 s.	
Distribution enligt missiv	Pris: Enligt prislista	

